horticulturae

MDPI

Article

Cold Plasma Treatment Alters the Morphology, Oxidative Stress Response and Specialized Metabolite Content in Yellow Iris (*I. reichenbachii*) Callus

Slađana Jevremović [1,*], Milica Milutinović [1], Ksenija Veličković [2], Uroš Gašić [1], Nikola Škoro [3], Nevena Puač [3] and Suzana Živković [1,*]

[1] Department of Plant Physiology, Institute for Biological Research "Siniša Stanković"—National Institute of the Republic of Serbia, University of Belgrade, Bulevar Despota Stefana 142, 11108 Belgrade, Serbia; milica.milutinovic@ibiss.bg.ac.rs (M.M.); uros.gasic@ibiss.bg.ac.rs (U.G.)
[2] Faculty of Biology, University of Belgrade, Studentski Trg 16, 11158 Belgrade, Serbia; ksenija@bio.bg.ac.rs
[3] Center for Non-Equilibrium Processes, Institute of Physics, National Institute of Republic of Serbia, University of Belgrade, Pregrevica 118, 11080 Belgrade, Serbia; nikola.skoro@ipb.ac.rs (N.Š.); nevena.puac@ipb.ac.rs (N.P.)
* Correspondence: sladja@ibiss.bg.ac.rs (S.J.); suzy@ibiss.bg.ac.rs (S.Ž.)

Abstract

The application of non-thermal (cold) plasmas is considered an environmentally friendly method that could affect plant metabolism and cellular development or can be used for the commercial production of natural products that cannot be chemically synthesized. In the present study, the non-embryogenic callus of iris (*Iris reichenbachii* Heuff.) was treated with a Radio Frequency (RF) plasma needle device using He as a working gas. We investigated short-term (up to seven days) and long-term (up to one year) changes on morphological, physiological and biochemical levels. An increased production of O_2^- and H_2O_2 was observed in the callus tissue after plasma treatment. The enzymes SOD and CAT represented the frontline in the antioxidant defense against reactive oxygen species (ROS) produced during the first hour of treatment, while POX was the leading antioxidant enzyme seven days after plasma treatment. Significant long-term morphological changes were observed in the calli due to the increased mitotic activity of the plant cells. In addition, three flavonoids (naringenin, apigenin and acacetin) and two isoflavonoids (irisolidone and irilone) were detected only in the plasma-treated tissue even one year after plasma treatment. The present study emphasizes the application of the plasma technique to promote meristematic activity and stimulate the production of specialized metabolites in iris calli.

Keywords: callus; iris; cold plasma; antioxidant activity; isoflavonoids

check for updates

Academic Editor: Yanyou Wu

Received: 27 May 2025
Revised: 21 June 2025
Accepted: 26 June 2025
Published: 3 July 2025

Citation: Jevremović, S.; Milutinović, M.; Veličković, K.; Gašić, U.; Škoro, N.; Puač, N.; Živković, S. Cold Plasma Treatment Alters the Morphology, Oxidative Stress Response and Specialized Metabolite Content in Yellow Iris (*I. reichenbachii*) Callus. *Horticulturae* **2025**, *11*, 781. https://doi.org/10.3390/horticulturae11070781

Copyright: © 2025 by the authors. Licensee MDPI, Basel, Switzerland. This article is an open access article distributed under the terms and conditions of the Creative Commons Attribution (CC BY) license (https://creativecommons.org/licenses/by/4.0/).

1. Introduction

Cold plasma (CP), also known as non-thermal or low temperature plasma, is an innovative technology that has wide range application in agriculture including seed germination, cultivation, surface sterilization, microorganism decontamination, food manufacturing processing and storage, wound healing, plant growth as well as secondary metabolite production [1]. Increasing interest for the application of CP lies in the fact that no expensive vacuum systems are required, the geometries of electrode systems are versatile and can be adapted depending on the type of samples and the desired characteristics of the plasma [2–4]. The main disadvantage of CP is the need for high-voltage power supplies

and, in most cases, the need for the addition of noble gases (Ar, He, etc.) that are used to lower the breakdown voltage. Both can increase the cost of plasma applications, but even with this, CP remains competitive with classical methods that involve the usage of additional chemical compounds or complicated processes. This is due to the most important feature of CPs—their rich chemistry [5,6]. There is some evidence that chemical species in the plasma, with ample amounts of reactive oxygen and nitrogen species (RONS), are responsible for triggering various mechanisms that affect the plant cells [6,7]. The demand for precise and localized in vivo treatments of living cells and tissues resulted in the fast development of various plasma devices that operate at atmospheric pressure [1,8,9]. The plasma sources have a variety of designs and operating procedures such as corona discharges, spark discharges, dielectric barrier discharges, or underwater discharges, with the plasma needle as one of the atmospheric pressure devices that meet the requirements for the precise and localized treatments of living cells and tissues [1,10].

Numerous studies have demonstrated that this modern eco-agricultural technology is effective in improving agronomic seed quality and has the potential to be used for seed decontamination, germination activation, and seedling growth [11–16]. A few reports have also investigated stressor-induced changes in physiological and biochemical activities, such as the amount of pigments and secondary metabolites, antioxidant capacity, and the regulation of photosynthesis [11,17,18]. There is a wealth of data on CP treatment that has been carried out on seeds and seedlings ex vitro (summarized in 1,7,19), and, in all cases, the results showed that CP treatment can increase the content of valuable secondary metabolites [19–23]. On the other hand, there are not as many reports on the effect of CP on plant material during cultivation in vitro, like calli culture [24,25], synthetic seeds [26], liverworts [27], or genome editing [28]. Direct plasma treatment has been shown to have significant long-term effects on callus growth in some ornamental plants with plasma-treated callus growing better than the untreated one [24,25]. Callus, as a growing mass of unorganized plant parenchyma cells, can also produce bioactive compounds. Over the last few decades, significant progress has been made in the production of these compounds using plant tissue culture techniques. There are many studies reporting the production of specialized metabolites in callus and/or differentiated tissue cultures with callus cultures being the preferred in vitro culture system for achieving high yields and consistent material production for commercial use [29–33]. Recently, it has been reported that the CP treatment of calli can trigger the production of valuable secondary metabolites [10,34]. The authors showed that corona discharge plasma enhanced callogenesis and stimulated the production of cannabinoids in cannabis calli [34] and atropine in the callus of *Datura inoxia* [10]. It has also been suggested that, considering the necessity of keeping sterile conditions, the development of new specialized devices is necessary to facilitate the application of plasma treatment in the field of plant tissue culture [10].

Irises, a group of plants from the family Iridaceae, have immense medicinal importance in addition to their ornamental value, as they contain a variety of valuable secondary metabolites [35], which are used in the treatment of cancer, inflammation, bacterial and viral infections summarized in the studies of [36–38]. Characteristic phytochemicals of irises are flavones, flavone C-glycosides, isoflavones, terpenoids, xanthones, phenols, stilbenes, and quinones [39,40]. Of particular pharmaceutical interest are isoflavonoids, which are also characteristic of plants from the family Leguminosae. They represent the typical ecophysiological active compounds that act as defense substances and are mainly accumulated in the underground part of the plants. To date, 85 isoflavonoid aglicones and glycosides have been found in 18 different species belonging to the genus iris [41–44]. Most of them were isolated from the rhizome and leaves of the plant material collected in

nature and showed antioxidant, anti-inflammatory, antiviral, antibacterial and estrogen-like effects [38,45,46].

Plant tissue culture methods, including callus and in vitro shoot and root regeneration, can ensure the production of valuable secondary metabolites or raw materials in large quantities without destroying the natural habitat [47]. In the case of irises, plant regeneration in in vitro culture has been reported for many endemic, endangered, and threatened species [48–51], as well as for some ornamental [52–55] and pharmaceutically or perfumery valuable iris species [56–59]. The production of secondary metabolites in in vitro tissue culture has been investigated in several species of the genus iris (Table 1). In the culture of iris callus, cell suspensions or adventive roots, the production of flavones [60,61], isoflavones [62–64], irones [49,65], iridals [66,67], essential oils [68] and xanthones [63,69] was investigated. It should be emphasized that the yellow color of the iris callus is due to the accumulation of carotenoids and not xanthones [52,69]. So far, the isoflavonoid production ability of irises has been evaluated in adventive root cultures of *I. germanica* [62] and *I. pseudacorus* [64], shoot cultures of *I. sibirica* [63] and callus cultures of *I. pseudacorus* [70] and [*I. domestica* [71]. There are some data in the literature on elicitation of the production of secondary metabolites in iris during regeneration in tissue culture by varying different plant growth regulators in the culture medium [60,61,63] or by adding various abiotic elicitors, such as $CuCl_2$ [62], phenylalanine [70], jasmonic acid [72] or quinone [49]. In addition, some flavonoids were isolated from the callus tissue of *I. ensata* [61], which are uncharacteristic of intact plants collected in nature (Table 1).

Table 1. A list of specialized metabolites recorded during in vitro growth of irises.

Plant Species	Culture Type	Compound	Elicitation	References
Iris atrofusca	Callus	Irones Essential oils	Quinine	[49] [68]
Iris domestica	Callus	Isoflavonoids	$CuCl_2$	[71]
Iris ensata	Callus	Flavonoids Flavones		[60] [61]
Iris germanica	Root cultures Callus	Isoflavonoids Carotenoids	$CuCl_2$	[62] [73]
Iris pallida	Cell suspensions Leaves	Iridals		[66] [59]
Iris petrana	Callus	Irones Essential oils	Quinine	[49] [68]
Iris pseudacorus	Cell suspensions Callus Shoots, roots Root culture	Iridals Isoflavonoids Phenolics Isoflavones	Phenilalanine Jasmonic acid	[67] [70] [72] [64]
Iris reichenbachii	Callus, Shoots	Xanthone (Mangiferin)		[69]
Iris sibirica	Callus Cell suspension Shoots	γ irone Volatile oils Flavonoids Isoflavonoids Mangiferin	Auxin (NAA)	[65] [74] [75] [63] [76]

The subject of this study was *Iris reichenbachii* (Heuffel), dwarf bearded or yellow iris (Syn: *I. bosniaca* G. Back 1960, *I. balkana* Janka, 1960, *I. skorpilii* Velenovsky, *I. serbica* Pančić, 1856), which is an endemic plant and can be found in several locations on the Balkan Peninsula [77] (Figure 1a). So far, the synthesis of valuable xanthones (mangiferin, isomangiferin), flavones (apigenin, acacetin, chrysoeriol) and C-glycosylflavones (isoorientin, luteolin di-C-glycoside) was recorded mainly in leaves and rhizomes of this species [44,78–81]. Šavikin and coworkers showed that the isoflavonoid iridin was present in the rhizomes of *I. reichenbachii* collected in the wild [80]. In addition, Jevremović et al. [77,82,83] established a protocol for the in vitro regeneration of mature zygotic embryos of *I. reichenbachii* and investigated the production of mangiferin (C-flavone glycoside) during tissue culture induction and the plantlet regeneration of *I. reichenbachii* in vitro [69]. The authors stated that the synthesis of mangiferin was recorded during shoot regeneration, while, in callus culture, mangiferin was detected only in traces [69]. According to preliminary data, cold plasma may have some effects on callus growth as well as the production of secondary metabolites in iris calli, but the mechanism of plasma treatment-induced changes is not yet clear [84].

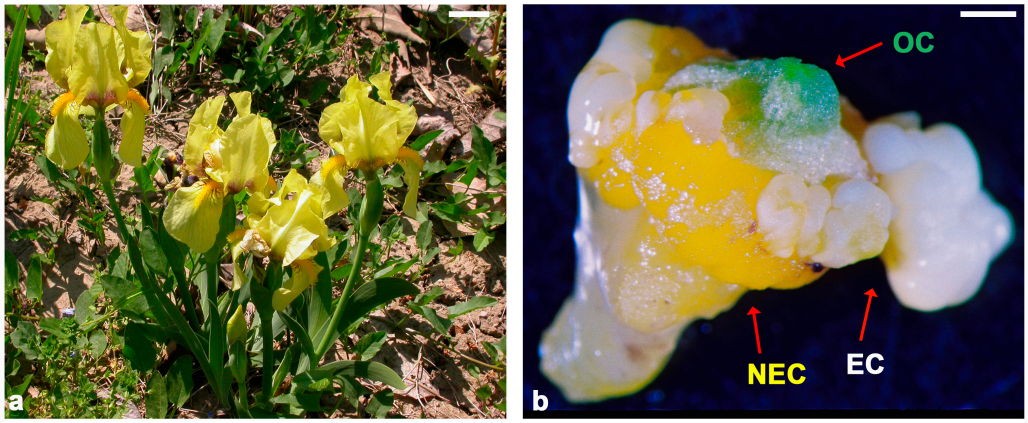

Figure 1. Dwarf iris, *Iris reichenbachii* (Heuffel): (**a**) Plants in natural habitat. (**b**) Three types of calli formed in the culture of zygotic embryos on a medium supplemented with 2,4-D: white, embryogenic (EC), green organogenic (OC) and yellow non-embryogenic (NEC) calli. Bars: (**a**) 10 mm; (**b**) 1 mm.

When in vitro cultures are induced on a 2,4-D containing medium, three types of calli can be distinguished in most iris species, including *I. reichenbachii* (Figure 1b) based on their color and consistency: (i) white calli, referred to as embryogenic calli (EC), (ii) green, organogenic calli (OC), and (iii) yellow referred to as non-embryogenic calli (NEC) [50,55,56,59,85,86]. After prolonged culture, yellow callus is often the most common and frequent, showing no morphogenetic response with very low regeneration potential, and therefore represents one of the greatest challenges in this field of research.

Accordingly, the present study aimed to complete the knowledge on the short- and long-term effects of CP on the yellow non-embryonic callus of *I. reichenbachii* at different levels: (i) morphological, (ii) histological and (iii) physiological, including the assessment of oxidative stress and antioxidant defense of calli immediately after plasma treatment. The long-term effects of plasma will focus on the ability of plasma priming to be used as an alternative tool/elicitor for the production of specialized metabolites in yellow iris calli.

2. Materials and Methods

2.1. Plant Material and Growth Conditions

For the experiments, a nodular, yellow non-embryogenic callus (NEC) of *I. reichenbachii* Heuff was used. Callus induction was performed in the culture of mature zygotic

embryos as described in the study of [77]. Three types of calli were initially induced: white embryogenic calli (EC), green organogenic calli (OC) and yellow non-embryogenic calli (NEC). All calli were grown on solid MS medium consisting of MS mineral solution [87], 3% sucrose, 250 mg of casein hydrolysate and 250 mg of proline, supplemented with 2,4-dichlorophenoxyacetic acid (2,4-D) and kinetin, 1.0 mg L^{-1} each and subcultured on fresh medium every four weeks. After several subcultures, the embryogenic potential decreased, and most calli became yellow nodular, slow-growing NEC. The yellow *I. reichenbachii* callus used in this work was maintained for several months prior to the experiments by transferring a portion of calli to the same medium. All cultures were grown at a temperature of 24 ± 2 °C and under a 16 h light/8 h dark photoperiod (photon flux density of 40 µmol m^{-2} s^{-1} provided by cool white fluorescent lamps).

2.2. Non-Thermal Plasma System and Treatment Conditions

A cold (non-thermal) atmospheric plasma source—plasma needle, which operates at a frequency of 13.56 MHz, was used for the treatment of iris calli (Figure 2a,b). It consisted of a central tungsten electrode (diameter 0.5 mm) enclosed in a ceramic tube and placed inside a glass tube (inner diameter 4 mm, outer diameter 6 mm). The body of the plasma needle was made of Teflon. Further details on the system can be found in [88]. The working gas was helium, and the flow was kept constant at 1 slm (standard liter per minute) in all experiments. At the end of the tube in the mixture of helium and ambient air, plasma was generated and enabled the formation of RONS important for the treatment of biological samples (Figure 2c). The power introduced into the plasma was monitored and did not exceed a few watts, which is another important factor for the treatment of sensitive samples.

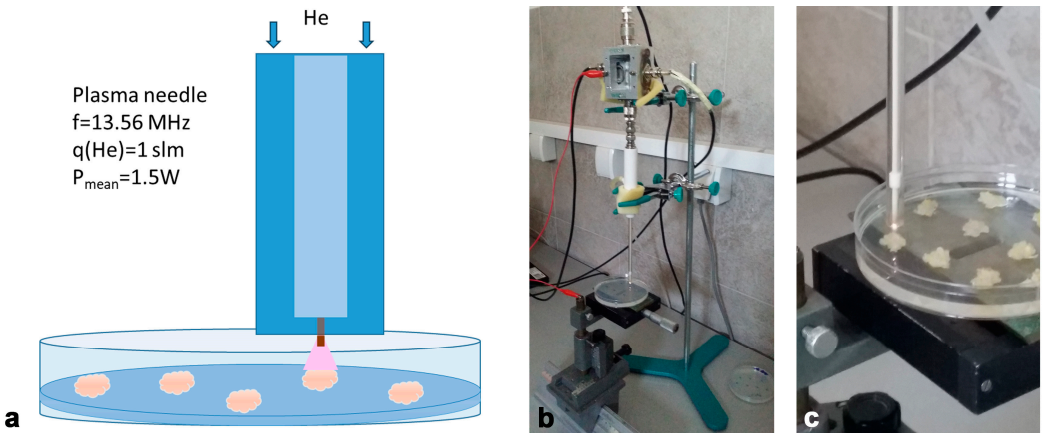

Figure 2. Plasma needle setup for the treatment of iris callus: (**a**) schematic illustration of cold atmospheric plasma (CP) treatment used in the experiments; (**b**) plasma needle device; (**c**) treatment of callus with plasma.

Ten calli samples (30–60 mg) were placed in a Petri dish containing 20 mL growth medium (MS medium with 2,4-D and kinetin, 1.0 mg L^{-1} each) before treatment with plasma. Plasma treatment was performed directly on the upper surface of callus using needle after uncovering the Petri dish. The treatment times were 10 s, 30 s and 60 s, at power deposited to the plasma of 1.5 W. All treatments were performed in triplicate. Untreated (control) calli samples were grown in a Petri dish filled with culture medium in the same way as the plasma-treated samples during the experimental procedure to ensure equal treatment conditions. After treatment, calli were either immediately frozen in liquid nitrogen and stored at −80 °C until use or continuously cultured in Petri dishes before use. The whole experiment was repeated twice.

2.3. Histological Analysis

The calli samples were fixed in FAA fixative (10% formalin, 5% acetic acid, 50% ethanol) at room temperature for 24 h. The fixed samples were dehydrated through a graded series of ethanol (50%, 70%, 96%, 100%), cleared in xylene and embedded in paraffin [89]. Tissue sections (10 µm) were routinely deparaffinized with xylene, rehydrated in graded ethanol, and stained with a 1% toluidine blue solution (Sigma-Aldrich, St. Louis, MO, USA). All sections were mounted in DPX mounting medium (Sigma-Aldrich, St. Louis, MO, USA) and examined using a DMLB microscope (Leica Microsystems, Wetzlar, Germany).

2.4. Histochemical Localization of O_2^- and Production of H_2O_2

The localization of superoxide anion radicals (O_2^-) and H_2O_2 was performed according to the modified method described in [90]. The formation of O_2^- was visualized using the reduction staining method of nitro blue tetrazolium (NBT, Sigma-Aldrich, St. Louis, MO, USA) as blue formazan precipitates due to the reduction in NBT in the presence of O_2^-. The control and treated calli samples were incubated in 2.5 mM NBT solution in 50 mM sodium phosphate buffer (pH 7.8) containing 10 nM of NaN_3 in the dark at room temperature for 2 h. Accumulation of H_2O_2 was detected by formation of a brown polymerization product after incubation of the calli with a 3,3′-diaminobenzidine (DAB, Sigma-Aldrich, St. Louis, MO, USA) solution (5 mM DAB-HCl, pH 3.8) for 2 h in the dark at room temperature. All samples were stored in a glycerol/ethanol solution (1:4; *v*/*v*) prior to light microscopic analysis and visualized with a Leica DMLB 2900 light microscope (Leica Microsystems, Wetzlar, Germany) using the LAS V4.11 program.

2.5. Protein Extraction

Yellow callus samples (NEC, approximately 50 mg FW) were grounded in liquid nitrogen using a mortar and pestle and homogenized in 100 mM potassium phosphate buffer (pH 6.5) containing 1 mM of phenylmethylsulfonyl fluoride (PMSF), 2 mM of EDTA, 5 mM of ascorbic acid, 0.5% Tween-20 and 2% (*w*/*v*) polyvinylpolypyrrolidone (PVPP). The homogenates were centrifuged at 14,000 g for 20 min, at +4 °C. The supernatant was used for the assays. The total protein content in the extracts was determined using a Qubit 3.0 Fluorimeter (Life Technologies, Thermo Fisher Scientific, Waltham, MA, USA) according to the instructions of the Qubit protein assay kit (Thermo Fisher Scientific, Waltham, MA, USA).

2.5.1. Native-PAGE Electrophoresis and Determination of Enzyme Activity

Separation by native polyacrylamide gel electrophoresis (native-PAGE) and activity staining of SOD, CAT and POX isoforms were performed according to procedure reported in the study of [11,91].

2.5.2. SDS-PAGE Electrophoresis and Immunoblotting

Sodium dodecyl sulfate-polyacrylamide gel electrophoresis (SDS-PAGE) and subsequent transfer of proteins to nitrocellulose membranes were performed as reported by the authors of [91]. The primary antibodies used in this work were CSD2 antibody (Anti-Rabbit chloroplastic CuZn-Superoxide Dismutase, AS06170; Agrisera Antibodies, Vännäs, Sweden), Anti-Rabbit Mn-Superoxide Dismutase antibody (AS09524, Agrisera Antibodies, Sweden), Anti-Catalase antibody (1:1000, AS09501; Agrisera Antibodies, Sweden), Anti-Peroxidase (AS09548, Agrisera Antibodies, Sweden) and goat Anti-Rabbit IgG peroxidase (A0545, Sigma-Aldrich, Saint Louis, MI, USA) as secondary antibodies. After intensive washing in the PBS buffer, the protein signals were visualized using an enhanced chemiluminescence detection (ECL) system. Densitometry analysis of band intensities was

performed using ImageJ 1.32j software (W. Rasband, National Institute of Health, Bethesda, MD, USA). The signal intensities obtained were normalized to the value of the control sample, and the results are presented as relative abundances.

2.6. Preparation of the Extracts

Control (NEC and EC) and plasma-treated calli samples (30–50 mg) were ground to a fine powder with liquid nitrogen and extracted using methanol (1:10, *w*:*v*) at room temperature. After a short 10 min sonication in ultrasonic water bath (Sonorex Bandelin Electronic, Berlin, Germany), the extracts were centrifuged at 12,000 g for 20 min. The supernatants were filtered with 0.2 µm cellulose filters (Agilent Technologies, Santa Clara, CA, USA) and stored at +4 °C until use.

2.7. UHPLC-LTQ Orbitrap MS Analysis

The compounds of interest were separated using an Accela 600 ultra-high-performance liquid chromatography (UHPLC) system coupled to a linear ion trap—Orbitrap mass spectrometer (LTQ OrbiTrap MS; ThermoFisher Scientific, Bremen, Germany). A Syncronis C18 column (100 × 2.1 mm, 1.7 µm particle size) thermostatted at 40 °C was used to separate the compounds. The flow rate was set to 300 µL min^{-1}, and the mobile phase consisted of 0.1% formic acid in water (A) and acetonitrile + 0.1% formic acid (B). The injection volumes were 5 µL. The linear gradient program used for sample analysis was described in detail in the study of [92]. The MS was equipped with a heated electrospray ionization probe (HESI-II, Thermo Fisher Scientific, Bremen, Germany) operating in negative ionization mode. The MS spectra were acquired by full-range acquisition over 100–1000 m/z. The parameters of the ion source and the other MS settings were the same as previously described by the study of [93]. Xcalibur software (version 2.1) was used for instrument control, data acquisition, and analysis. Identification of unknown compounds was performed by exact mass search of their deprotonated molecule ($[M-H]^-$) and their MS^4 fragmentation, as well as by literature search of available chromatographic and MS data [41,94–97].

2.8. Statistical Analysis

Statistical analyses were performed using STATGRAPHICS software, v. 4.2 (Statgraphics Technologies, Inc., The Plains, VA, USA). Data were subjected to analysis of variance (ANOVA), and comparisons between the mean values of treatments were performed using Fisher's Least Significant Difference (LSD) post hoc test at a confidence level of $p < 0.05$ and $p < 0.01$.

3. Results

We evaluated the morphological (Section 3.1) and histological (Section 3.2) changes, as well as the oxidative stress assessment (Section 3.3) of yellow iris calli immediately after the plasma treatment of 10 s, 30 s, and 60 s (marked as 0 h time point), as well as one hour (1 h) and seven days (7d) after treatment. In addition, pronounced morphological changes and the development of white calli were observed only on samples after plasma treatment for 60 s. Therefore, long-term changes in phytochemical profile in plasma-treated (60 s) in comparison to untreated iris calli were evaluated after one week, three weeks and one year of cultivation following plasma treatment (Section 3.4).

3.1. Morphological Changes in Iris Calli After Plasma Treatment

After plasma treatment, all treated calli samples continued to grow on the same culture medium as untreated calli (Figure 3). It should be emphasized that there were no signs of plant material contamination, although the plasma needle setup and treatments were not performed under aseptic conditions (Figure 2). The first clearly visible mor-

phological changes after the CP treatment were observed on the surface of treated calli (Figure 3b–h). Untreated calli had a compact nodular structure with a smooth surface (Figure 3a). Morphological change was recorded 7 days after plasma treatment, when a mucilaginous envelope around the plasma-treated calli samples was observed (Figure 3 b–d). After three weeks, the nodular structure disorganized, and protrusions of white calli appeared on the surface of the nodules (Figure 3e–g). It was also noted that the plasma-treated iris calli grew better after prolonged culture in comparison to untreated calli (Figure 3i).

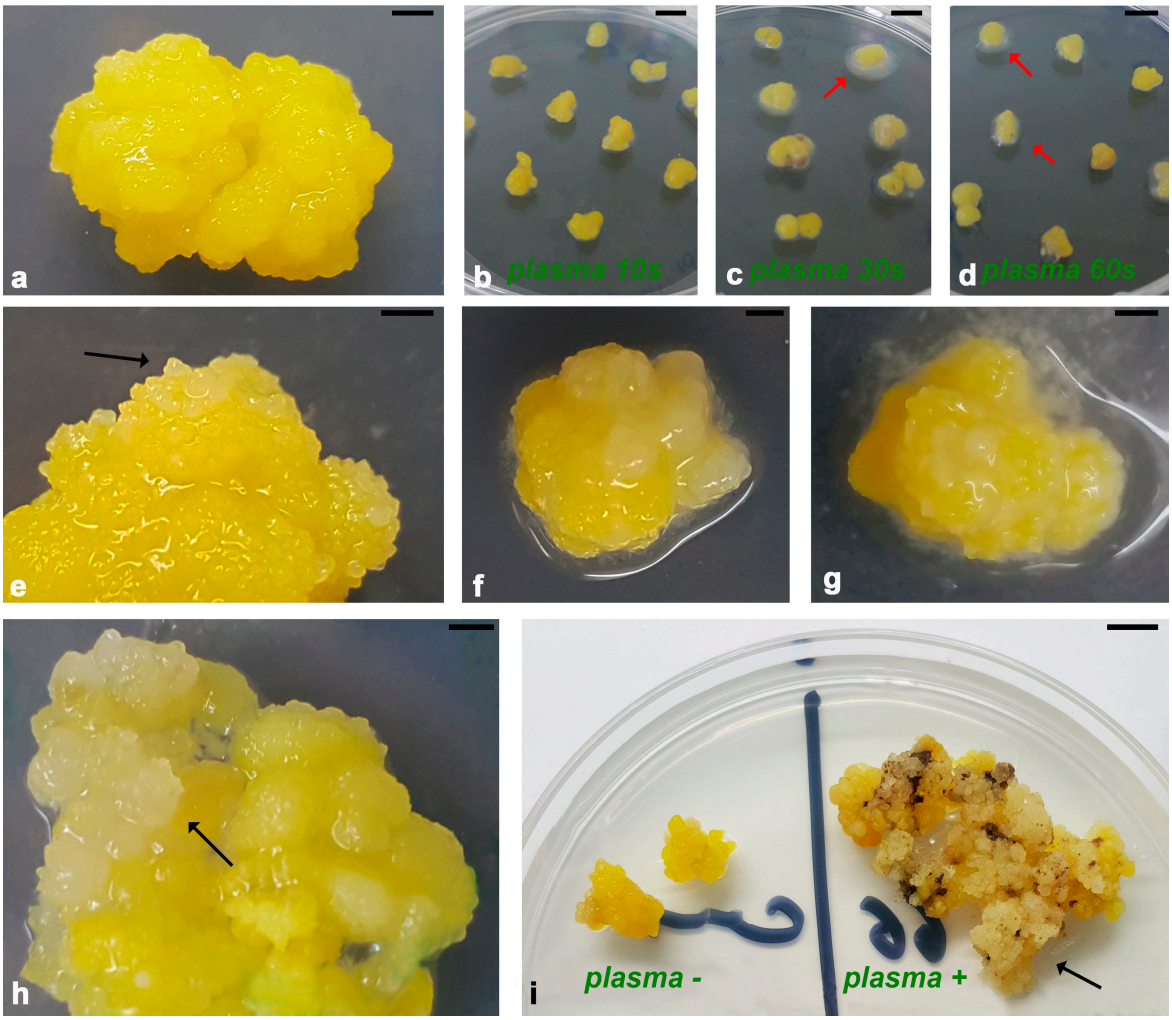

Figure 3. Morphological changes in iris calli after plasma treatment: (**a**) Untreated iris callus. (**b**–**d**) Calli samples 7 days after plasma treatment for 10 s (**b**), 30 s, (**c**) and 60 s (**d**). (**e**–**h**) Development of white calli on plasma-treated samples (60 s) three weeks after the treatment. (**i**) Calli cultures ten weeks after plasma treatment for 60 s (left—untreated calli; right—plasma-treated calli; note: growth of plasma-treated calli). The red arrows indicate the formation of mucilaginous "shell" around the callus; the black arrows indicate the formation of white callus on the surface of the treated calli. Bars: (**a**,**e**,**f**,**g**,**h**) 1 mm; (**b**,**c**,**d**) 5 mm; (**i**) 10 mm.

3.2. Histological Study of Iris Callus After PLASMA Treatment

Light microscopic examination revealed different cell types in the iris callus (Figure 4). The uniform cells were found in the untreated iris callus, where numerous parenchymatous cells (PCs) with a large vacuole, a thin cytoplasmic ring, and nuclei close to the cell wall were predominant (Figure 4a,d). Small regions in the inner parts of the untreated callus were characterized by tiny cells with a poorly developed vacuole system, dense cytoplasm, and a prominent nucleus and were designated as meristematic centers (MCs). In comparison

to the untreated callus, the most prominent change observed in the CP-treated callus was related to meristematic cells. The areas with small and cytosol-rich cells in the plasma-treated calli appeared to be larger and more visible than those of the untreated callus (Figure 4b,e,f). In addition, the changes observed in the plasma-treated callus were also noted after one year of cultivation, with several regions of meristem initiation appearing (Figure 4c,g). Taken together, these results clearly showed that the cellular organization of the plasma-treated calli was significantly different from that of the untreated callus.

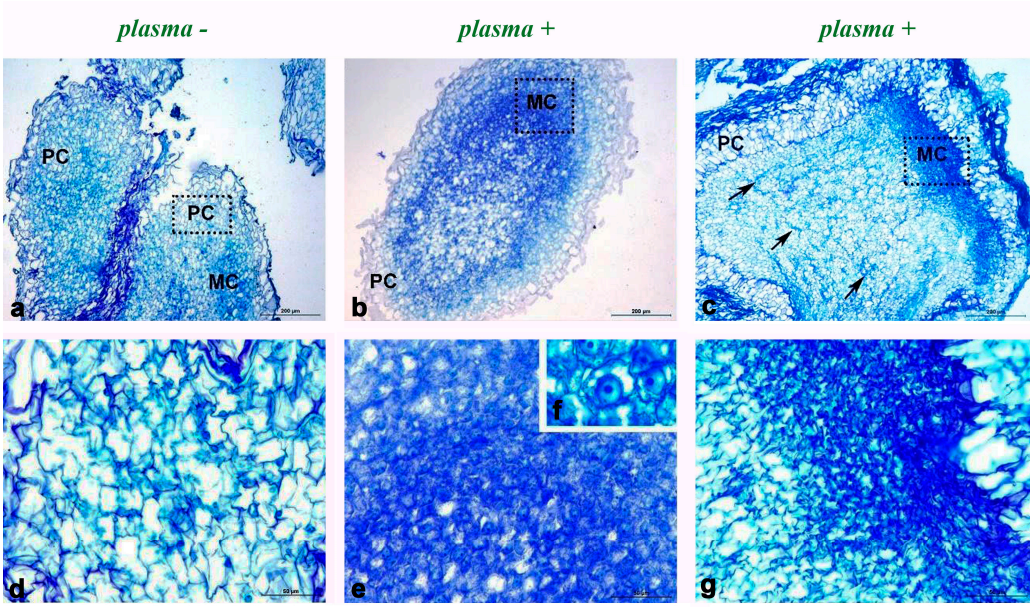

Figure 4. Histological study of *Iris reichenbachii* yellow callus treated with CP for 60 s: (**a**–**c**) Toluidine blue-stained cross-sections of untreated callus (**a**) and plasma-treated (**b**,**c**). (**d**) Detail of parenchymatous tissue of untreated callus. (**e**,**f**) Detail of meristematic center with typical meristematic cell (**f**) in plasma-treated calli. (**g**) Detail of cross-section of treated callus one year after plasma treatment for 60 s. Arrows indicate meristem initiation. Enlarged black dotted squares show typical histological features of parenchymatous cells (PCs) and meristematic cells in the meristematic center (MC). Bars: (**a**–**c**) 200 µm, (**d**–**g**) 50 µm.

3.3. Oxidative Stress Response of Iris Calli to Plasma Treatment

In order to investigate the oxidative stress response of iris callus to plasma treatment we evaluated the localization of reactive oxygen species (O_2^- and H_2O_2) production on the surface of the callus immediately after plasma treatment, one hour and one week after plasma treatment (Section 3.3.1). In addition, the activity (Section 3.3.2) and protein abundance of antioxidant enzymes (Section 3.3.3) were examined in parallel, during the same time periods.

3.3.1. Histochemical Localization of O_2^- Production and H_2O_2 Accumulation in Iris Calli After Plasma Treatment

Immediately after plasma treatment, an oxidative burst was observed on the surface of the iris yellow callus (Figure 5a–h). The production of oxygen anion (O_2^-) was localized mainly in cell walls and the extracellular matrix, outside of cells on untreated callus samples (Figure 5a,e), while in the plasma-treated callus, all surfaces of the callus were intensively stained with NBT (Figure 5b). In the cross-section, it was obvious that the increased production of oxygen anion was localized on the surface of the callus nodule (Figure 5f). In parallel, the accumulation of H_2O_2 was also recorded on the surface of the iris callus after plasma treatment (Figure 5d). In untreated calli, the accumulation of H_2O_2 was recorded sporadically around individual cells inside the callus (Figure 5g), while, in

the plasma-treated callus, significant accumulation of brown DAB staining, indicating increased accumulation of H_2O_2, was observed at the surface of the callus (Figure 5h).

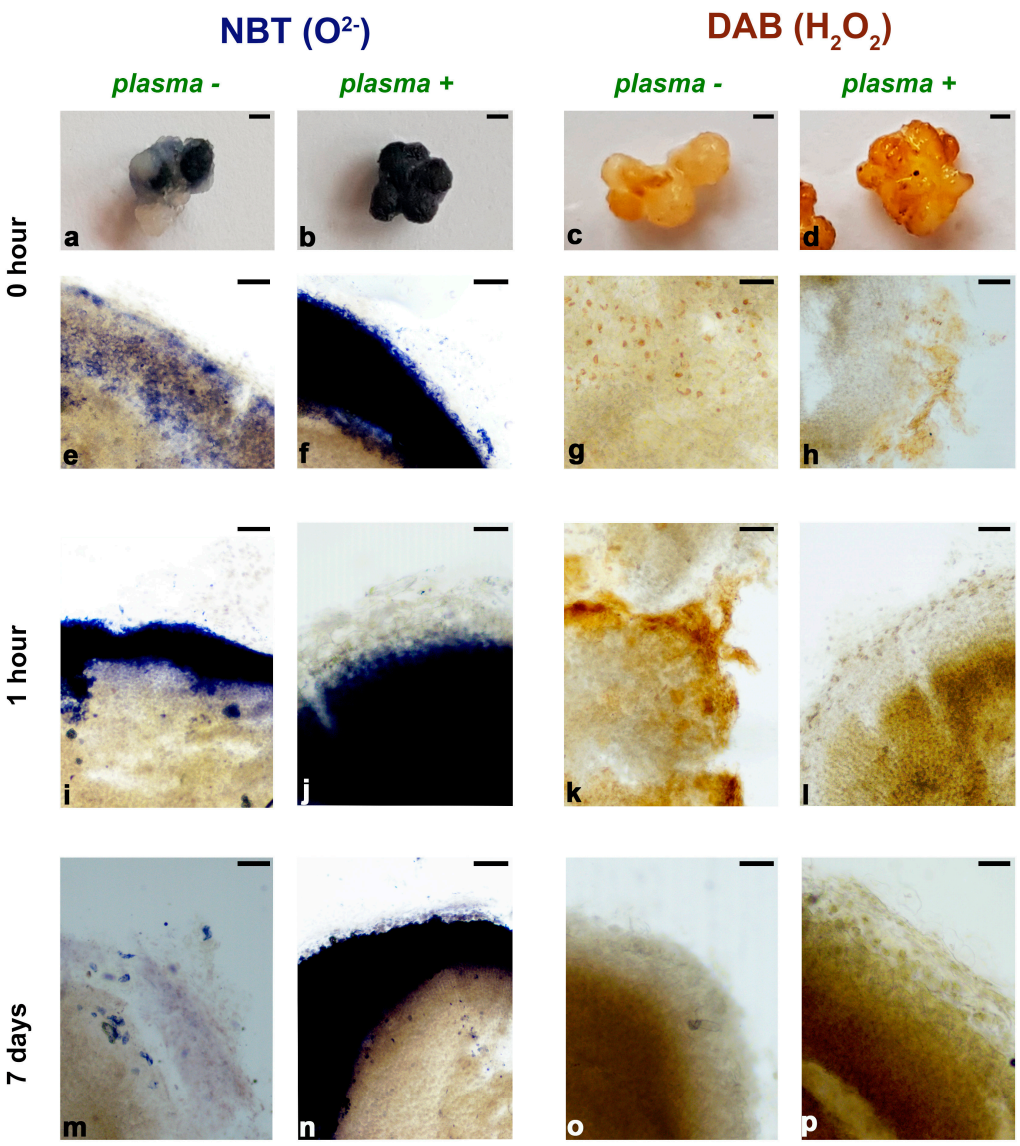

Figure 5. Histochemical localization of oxygen anion (O_2^-) and hydrogen peroxide (H_2O_2) production in *Iris reichenbachii* callus treated with plasma. Plasma-untreated and treated calli samples stained with NBT (**a**,**b**) and DAB (**c**,**d**) immediately after plasma treatment (0 h); cross-sections of untreated and CP-treated calli immediately after plasma treatment, 1 h and 7 days after plasma treatment. NBT staining (**e**,**f**,**i**,**j**,**m**,**n**); DAB staining (**g**,**h**,**k**,**l**,**o**,**p**). Bars: (**a**–**d**) 1 mm; (**e**–**p**) 200 µm.

One hour after plasma treatment, a significant increase in ROS production and accumulation of H_2O_2 was observed inside the callus (Figure 5j,l) in comparison to the untreated callus, where ROS production and H_2O_2 accumulation were detected on the surface of the iris callus (Figure 5i,k). Seven days after plasma treatment, an oxidative burst was noticed on the surface of plasma-treated callus (Figure 5n) compared to the untreated samples (Figure 5m). In contrast to O_2^- production, the H_2O_2 accumulation 7 days after plasma treatment was localized inside the callus nodule of both the untreated (Figure 5o) and treated callus (Figure 5p). However, cell layers with different DAB staining intensities (light and strong) were detected from the surface to the center of the callus nodule in the plasma-treated calli (Figure 5p).

3.3.2. Activity of Antioxidant Enzymes in Iris Calli After Plasma Treatment

Our results demonstrated that SOD and CAT in yellow iris calli were considered as the main enzymatic frontline in the antioxidant defense against ROS generated by plasma treatment (Figure 6). These enzymes showed a significant increase in total activity in response to CP treatment immediately and one hour after the plasma treatment (Figure 6a–c).

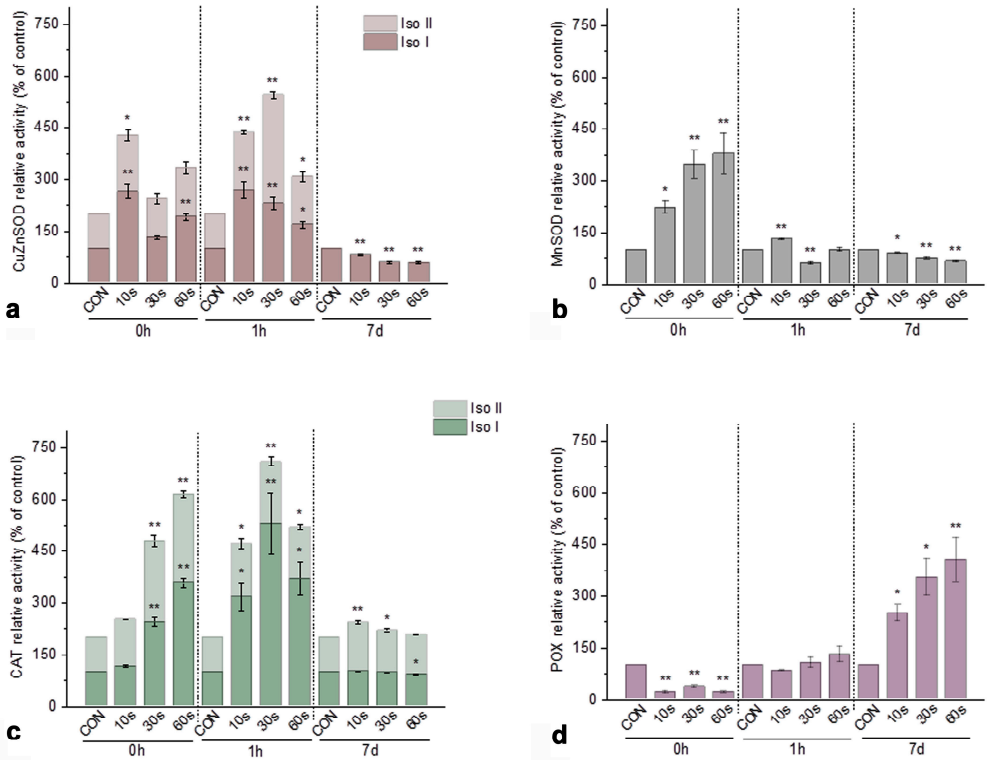

Figure 6. Activity of the antioxidant enzymes in *I. reichenbachii* callus after plasma treatment: (**a**,**b**) SOD activity, CuZnSOD (**a**), MnSOD (**b**); (**c**) CAT activity; (**d**) POX activity. Enzyme activities are measured immediately (0 h), one hour (1 h), or seven days (7d) of control (CON) and after CP treatment for 10 s, 30 s and 60 s. The band volume is determined by densitometric analysis. Data are normalized using the control signal. Values are means ± SE from two independent experiments. The asterisk indicates statistical significance compared to the control (* $p < 0.05$ and ** $p < 0.01$). Abbreviations: Iso I—Isoform I and Iso II—Isoform II.

Electrophoretic analyses of the SOD isoenzymes that were active and reacted after plasma treatment revealed three bands characterized as two CuZnSOD isoforms (Iso I and Iso II, Figure 6a) and one isoform of MnSOD (Figure 6b). The total CuZnSOD activity increased 1.5- to 3-fold in all plasma-treated samples collected immediately (0 h) and one hour (1 h) after treatment, respectively, compared to the untreated control sample (CON). Seven days (7d) after plasma treatment, total CuZnSOD activity decreased below baseline levels in all treated samples (Figure 6a). Contrary to CuZnSOD activity, a 2-4-fold increase in MnSOD activity was observed only immediately after plasma treatment (Figure 6b), which was below baseline one hour after plasma treatment. Seven days (7d) after plasma treatment, MnSOD isoforms showed a significant decrease in activity in comparison to untreated callus samples (Figure 6b).

A statistically significant increase in the activity of both detected CAT isoforms (Iso I and Iso II) was observed in all plasma-treated samples compared to the control (Figure 6c). Contrary to SOD and CAT, POX activity was significantly reduced immediately after treatment (0 h) compared with the control. In addition, POX activity in calli samples collected one hour (1 h) after treatment was not affected by low-temperature plasma

treatment. Seven days (7d) after plasma treatment, POX becomes the leading antioxidant enzyme that protects the iris callus from excessive ROS production in callus cells. POX activity increased with prolonged plasma treatment and reached the highest value after 60s of plasma treatment where POX activity was increased more than fourfold compared to the control untreated samples (Figure 6c).

3.3.3. Immunoblot Analysis of Antioxidant Enzymes in Iris Calli After Plasma Treatment

The protein level of the antioxidant enzyme isoforms was evaluated by immunoblot analysis with specific antibodies (Figure 7). Immunoblot analysis revealed the presence of a CuZnSOD band with a molecular weight of 19 kDa in all samples (Figure 7a). The intensity of the band corresponding to the CuZnSOD isoform appeared to decrease significantly in all treatments compared to the control untreated samples. A sharp decline in CuZnSOD protein level (up to three-fold) was observed immediately and 1 h after the 60 s plasma treatment. Immunoblot analysis revealed a band of 50 kDa in iris calli that corresponded to MnSOD (Figure 7b). In contrast to CuZnSOD, MnSOD protein levels showed a similar pattern to CAT in all treatments (Figure 7c), characterized by the positive correlation between total enzyme activity and abundance in samples collected immediately after plasma treatment (Figure 7b,c). MnSOD protein levels (Figure 7b) 1 h and 7d after plasma treatment resulted in an increase in protein level, but activity analysis showed a statistically significant decrease compared to control samples (Figure 7b).

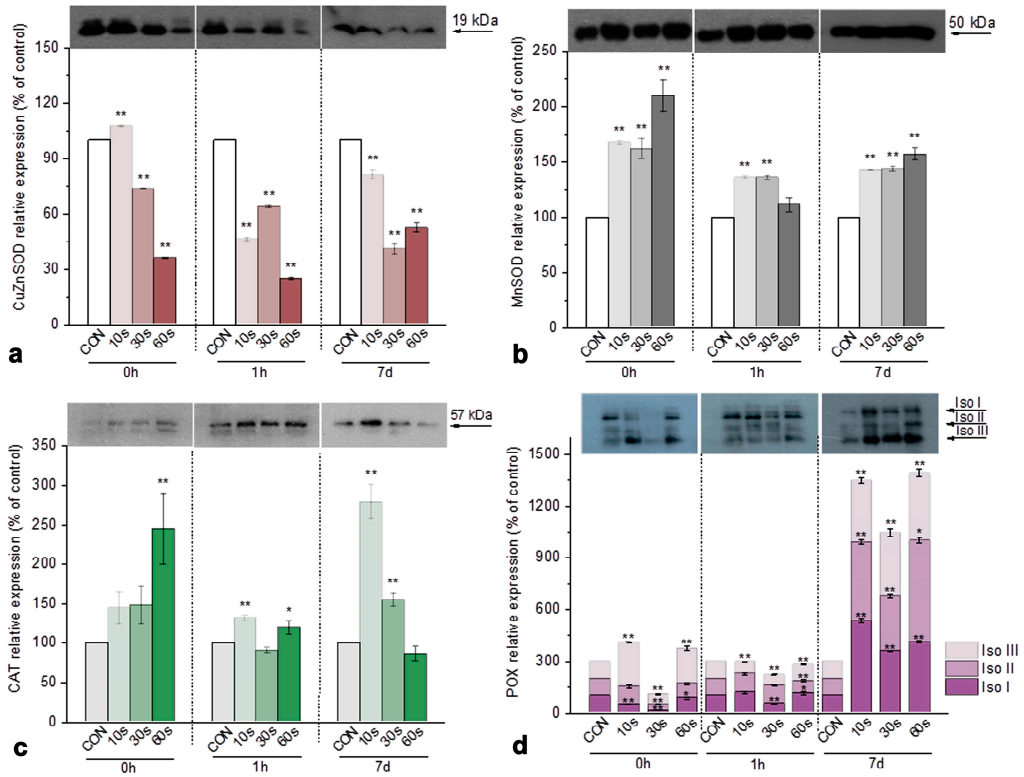

Figure 7. Immunoblot analysis of *I. reichenbachii* callus after plasma treatment: (**a**,**b**) SOD, (**a**) CuZn-SOD, (**b**) MnSOD, (**c**) CAT, (**d**) POX measured immediately (0 h), one hour (1 h), or seven days (7d) of control (CON) and CP treatment (10 s, 30 s and 60 s). The band volume was determined by densitometric analysis. Data are normalized using the control signal. Values are means ± SE obtained from two independent experiments. The asterisk indicates statistical significance compared to the control (* $p < 0.05$ and ** $p < 0.01$). Abbreviations: Iso I—Isoform I, Iso II—Isoform II and Iso III—Isoform III.

A single band of approximately 57 kDa, corresponding to CAT, was present in all samples. Excessive ROS accumulation leading to oxidative stress resulted in an increase in CAT protein content in all plasma-treated samples immediately after the treatment, with the highest values after the 60 s treatment compared to the control untreated samples (Figure 6c). Furthermore, the enhanced CAT protein content at 0 h, 1 h and 7d was consistent with the increase in enzyme activity at the same time points, as shown in Figure 5c. The physiological response of plasma-treated iris calli measured immediately after plasma treatment (0 h), 1 h and 7d after plasma treatment was characterized by an increase in POX protein content of all three observed isoforms compared to the control untreated callus (Figure 7d).

3.4. Secondary Metabolite Profile of Iris Calli Before and After Plasma Treatment

The UHPLC-Orbitrap-MS characterization of extracts from iris callus in negative ionization mode resulted in the detection of a total of 40 compounds. The identified compounds can be categorized into four structurally distinct groups: flavonoids and their derivatives (4 compounds), isoflavone glycosides (20 compounds), isoflavone aglycones (13 compounds) and 3 other compounds (Table 2). All detected compounds were identified by an exact mass search of their deprotonated molecule $[M–H]^-$, MS^{2-}, MS^{3-} and MS^4-fragmentation behavior and by comparison with the available literature. The peak numbers, compound names, retention times (t_R, min), molecular formulas, calculated and exact masses ($[M–H]^-$, m/z), and the presence of selected compounds in various cold plasma-treated calli samples are summarized in Table 2, while parent and major MS^2, MS^3, and MS^4 fragmentations are given in Supplementary Table S1.

Isoflavones and their glycosides and aglycones are the major classes of polyphenolic compounds found in the yellow callus of *Iris reichenbachii*. One flavonoid, six isoflavone aglycones, and eleven isoflavone glycosides were detected in the untreated yellow callus (NEC). On the other hand, the secondary metabolite profile of the untreated EC callus was characterized by eight isoflavonoid aglycones, ten isoflavonoid glycozides, three acetylated sucrose derivatives and other compounds, such Shengasu C, its isomer and diferuloylsucrose. The overall profile of secondary metabolites in iris callus changed with plasma treatment. De novo synthesis of three flavonoids (narigenin, apigenin, and acacetin) and two isoflavonoid aglycones (irisolidone and irilone) was detected only in plasma-treated iris calli (Table 2, purple). These compounds were not present in the untreated iris callus (NEC and EC) but were also recorded in CP-treated calli subcultured for one year after plasma treatment (Table 2). In addition, two isoflavone glycosides, irisolone 4′-O-(6′′-rhamnosyl)-hexoside and iriflogenin 4′-O-(6′′-hexosyl)-hexoside, were not recorded in plasma-treated or in untreated EC callus (Table 2, light blue). One year after plasma treatment, most of the isoflavone glycosides and aglycones that were present in the untreated callus were not detected in CP-treated calli (Table 2).

Table 2. Comparative analysis of high-resolution MS recorded secondary metabolite compounds in the untreated and treated callus of *I. reichenbachii* 7 days (1w), 3 weeks and 1 year (1y) after plasma treatment. Marked in purple—de novo synthetized compounds in plasma-treated callus; marked in green: compounds present in plasma-untreated and plasma-treated callus; and marked in blue: compounds present only in non-embryonic calli.

No	Compound name	t_R * (min)	Molecular Formula $[M–H]^-$	Calculated Mass $[M–H]^-$	Exact Mass $[M–H]^-$	Δ ppm	NEC **	PLASMA			EC
								1W	3W	1Y	
	Flavonoids and derivatives										
1	Apigenin 6-C-hexoside-8-C-pentoside	5.91	$C_{26}H_{27}O_{14}^-$	563,14063	563,13940	2.18	+	+	+	–	–
2	Naringenin	9.46	$C_{15}H_{11}O_5^-$	271,06120	271,06000	4.43	–	+	+	+	–
3	Apigenin	9.49	$C_{15}H_9O_5^-$	269,04554	269,0,474	2.97	–	+	+	+	–
4	Acacetin	11.80	$C_{16}H_{11}O_5^-$	283,06119	283,06110	0.32	–	+	+	+	–
	Isoflavone glycosides										
5	Tectoridin (Tectorigenin 7-O-hexoside)	5.93	$C_{22}H_{21}O_{11}^-$	461,10894	461,10894	−0.01	+	+	+	–	+
6	Iristectorin B (Iristectorigenin B 7-O-hexoside)	6.14	$C_{23}H_{23}O_{12}^-$	491,11950	491,11961	−0.23	+	+	+	–	+
7	Irislactin A	6.21	$C_{40}H_{47}O_{22}^-$	879,25645	879,25719	−0.84	–	–	–	–	+
8	Acetylated sucrose derivative 1	6.26	$C_{41}H_{49}O_{23}^-$	909,26701	909,26698	0.04	–	–	–	–	+
9	Isotectorigenin 7-O-hexoside	6.37	$C_{22}H_{21}O_{11}^-$	461,10894	461,10919	−0.55	–	–	–	–	+
10	Iridin (Irigenin 7-O-hexoside)	6.42	$C_{24}H_{25}O_{13}^-$	521,13007	521,13006	0.01	+	+	+	–	+
11	Homotectoridin (Homotectorigenin 7-O-glucoside)	6.52	$C_{23}H_{23}O_{12}^-$	491,11950	491,11987	−0.75	–	–	–	–	+
12	Isoridin (Isoirigenin 7-O-hexoside)	6.82	$C_{24}H_{25}O_{13}^-$	521,13007	521,13007	0.00	–	–	–	–	+
13	Acetylated sucrose derivative 2	7.05	$C_{45}H_{53}O_{25}^-$	993,28814	993,28742	0.73	–	–	–	–	+
14	Iristectorin A (Iristectorigenin A 7-O-hexoside)	7.27	$C_{23}H_{23}O_{12}^-$	491,11950	491.11764	3.79	+	+	+	–	+
15	Iridin S (Irisjaponin B 7-O-hexoside)	7.34	$C_{25}H_{27}O_{13}^-$	535,14572	535.14559	0.24	+	+	+	–	+
16	Irisolone 4′-O-(6′′-rhamnosyl)-hexoside	7.52	$C_{29}H_{31}O_{15}^-$	619,16684	619,16681	0.05	+	–	–	–	–
17	Irilone 4′-O-(6′′-hexosyl)-hexoside	7.54	$C_{28}H_{29}O_{16}^-$	621,14611	621,14423	3.03	–	–	–	–	–

Table 2. *Cont.*

No	Compound name	t_R * (min)	Molecular Formula $[M–H]^-$	Calculated Mass $[M–H]^-$	Exact Mass $[M–H]^-$	Δ ppm	NEC **	PLASMA			EC
								1W	3W	1Y	
18	Iriflogenin 4′-O-(6′′-hexosyl)-hexoside	7.60	$C_{29}H_{31}O_{17}^-$	651,15667	651,15625	0.65	+	–	–	–	–
19	Acetylated sucrose derivative 3	7.87	$C_{46}H_{53}O_{25}^-$	1005,28,814	1005,28768	0.46	–	–	–	–	+
20	Iristectorigenin A/B 7-O-(acetyl)hexoside	7.88	$C_{25}H_{25}O_{13}^-$	533,13006	533,13006	0.00	+	+	+	–	–
21	Acetylated sucrose derivative 4	7.90	$C_{47}H_{55}O_{26}^-$	1035,29871	1035,29881	−0.10	–	–	–	–	+
22	Irisolone 4′-O-[6′′-(3-hydroxy-3-methylglutaryl)]-hexoside	8.30	$C_{29}H_{29}O_{15}^-$	617,15119	617,15070	0.79	+	+	+	–	–
23	Iriskashmirianin 4′-O-[6′′-(3-hydroxy-3-methylglutaryl)]-hexoside	8.32	$C_{30}H_{31}O_{16}^-$	647,16176	647,16138	0.59	+	+	+	–	–
24	Iriflogenin 4′-O-[6′′-(3-hydroxy-3-methylglutaryl)]-hexoside	8.90	$C_{29}H_{29}O_{16}^-$	633,14611	633,14349	4.14	+	+	+	–	–
	Isoflavone aglycones										
25	Iristectorigenin A	6.34	$C_{17}H_{13}O_7^-$	329,06668	329,06688	−0.62	–	–	–	–	+
26	5,7,4′-Trihydroxy-6,3′,5′-trimethoxyisoflavone	6.47	$C_{18}H_{15}O_8^-$	359,07724	359,07718	0.17	–	–	–	–	+
27	Irisolone	7.71	$C_{17}H_{11}O_6^-$	311,05611	311,05545	2.12	+	+	+	–	–
28	Noririsflorentin	7.88	$C_{19}H_{15}O_8^-$	371,07724	371,07657	1.81	+	+	+	–	–
29	Tectorigenin	8.01	$C_{16}H_{11}O_6^-$	299,05611	299,05605	0.20	+	+	+	–	+
30	Dalspinosin	8.17	$C_{18}H_{15}O_7^-$	343,308233	343,08127	3.09	+	+	+	–	–
31	Iristectorigenin B	8.19	$C_{17}H_{13}O_7^-$	329,06668	329,06667	0.02	–	–	–	–	+
32	Irigenin	8.33	$C_{18}H_{15}O_8^-$	359,07724	359,07715	0.24	+	+	+	+	+
33	8-Hydroxyirigenin	8.33	$C_{18}H_{15}O_9^-$	375,07216	375,07214	0.05	–	–	–	–	+
34	Iristectorigenin A/B	9.93	$C_{17}H_{13}O_7^-$	329,06668	329,06592	2.31	+	+	+	+	+
35	Isoirigenin	9.97	$C_{18}H_{15}O_8^-$	359,07724	359,07731	−0.18	–	–	–	–	+
36	Irisolidone	10.89	$C_{17}H_{13}O_6^-$	313,07176	313,07166	0.32	–	+	+	+	–
37	Irilone	11.19	$C_{16}H_9O_6^-$	297,04046	297,04046	0.00	–	+	+	+	–
	Other compounds										
38	Diferuloylsucrose	6.04	$C_{32}H_{37}O_{17}^-$	69,320,362	69,320,357	0.07	–	–	–	–	+
39	Shegansu C	8.19	$C_{44}H_{47}O_{21}^-$	91,126,153	91,126,037	1.28	–	–	–	–	+
40	Shegansu C isomer	8.47	$C_{44}H_{47}O_{21}^-$	91,126,153	91,126,104	0.55	–	–	–	–	+

* tR–retention time; ** NEC–untreated non-embryonic calli of *I. reichenbachii* (control); 1W–plasma-treated NEC 7 days (one week) after plasma treatment for 60 s; 3W–plasma-treated NEC three weeks after plasma treatment for 60 s; 1Y-newly formed white calli of *I. reichenbachii* one year after plasma treatment for 60 s; and EC–white non-treated embryogenic calli of *I. reichenbachii*.

4. Discussion

To date, a variety of cold plasma devices with different designs and operating procedures have been developed that can generate and deliver plasma-reactive species to seeds, plants, soil, or water [1]. However, not as many devices have been used for in vitro cultures, especially for callus tissue grown under aseptic conditions [10,34]. In some recently published reports, corona discharge plasma was used to treat samples placed in covered Petri dishes [10], or calli simples were treated under sterile conditions [34]. The effects of plasma treatment with a corona device were evaluated ten days or two weeks after treatment for *Cannabis* and *Datura inoxia* calli, respectively [10]. In the present study, we exposed *Iris reichenbachii* calli to a low-temperature plasma treatment by using a plasma needle. The plasma needle generates a gas-phase chemistry rich in RONS [2,6,25,98]. During the experiments, the plasma comes into direct contact with the surface of the plant calli, where both short- and long-lived RONS can reach the plant cells and trigger various mechanisms of RONS defense response in callus cells. We presented here changes recorded immediately after plasma treatment, one hour and seven days after plasma treatment, as well as long-term effects that include changes in morphology and secondary metabolite content up to one year after plasma treatment.

According to the available research data, the plasma priming of calli efficiently improved callus biomass production [24,99]. The only long-term effects observed so far in plasma-treated calli were the increase in fresh weight of *Fritillaria imperialis* calli [24]. Similar results regarding the increase in callus growth were recorded in our study for the yellow non-embryogenic calli *of I. reichenbachi* [99]. Recently it was shown that all newly formed calli of *Datura inoxia* and *Cannabis sativa* exhibited vigorous growth after plasma treatment, but no change in calli color was observed [10,34].

Yellow callus types with a nodular structure can be formed in many iris species and are usually characterized as non-embryogenic calli (NEC) [85,100–102]. These types of calli are poorly granulated and water-stained compared to the embryogenic callus (EC), which is pale yellow or white and has a friable structure [102]. The non-embryogenic callus of *I. reichenbachii* is characterized by irregularly shaped cells containing minimal cytoplasm with light nuclear staining. After plasma treatment, we observed regions of smaller, densely packed meristematic cells that had a regular shape and a centrally located nucleus, suggesting that these cells have a strong meristematic potential. This type of cell was found only in friable, whitish calli, which consist of compact, glassy-like, embryogenic nodules that give rise to somatic embryos from the region of pro-embryonic meristematic cells. This type of calli is referred to in the literature as EC [85,100,102]. In the tissue culture of *I. germanica*, yellow callus covered with viscous substances is commonly referred to as callus, on which somatic embryos usually develop and become embryogenic when transferred to growth regulator-free MS medium [58]. In the iris, whitish plasma-derived calli obtained in this work did not further participate in embryogenesis and the development of somatic embryos. However, in our previous reports, we have shown that CP treatment induces the accumulation of arabinogalactan proteins (AGPs) on the surface of the nodules and in the extracellular mucilagenous part of the yellow iris calli [103]. AGPs are proteins that occur in the cell wall and in the extracellular space and represent specific markers for the transition of cells from the somatic to the embryogenic state [104]. The question remains whether the further development of somatic embryos in plasma-treated calli was only blocked because the calli were constantly grown on 2,4-D and KIN medium after CP treatment, which promotes callus development but not somatic embryo formation. Results obtained in this study showed that the surface modifications on the iris callus can be attributed to enhanced cell division (mitotic activity) and the development of new meristematic centers after CP treatment [105,106]. One of the reasons for the observed changes in the plasma-treated

iris calli could be related to the ability of plasma treatment to trigger the production of endogenous plant hormones. Therefore, the question of whether CP treatment also affects the hormonal status of iris calli needs to be further investigated.

To date, there is ample evidence that cold plasma-generated ROS and RONS play a crucial role in cell response [105–107]. Plasma treatment acts as an oxidative enhancer that disturbs the redox balance in plants, causing metabolic reactions and signaling cascades that consequently affect physiological and biochemical processes in plants [105,107]. In our study, we used two high-affinity probes (NBT and DAB) in iris calli samples after plasma treatment to provide information on the in situ site of formation and accumulation of ROS (O_2^- and H_2O_2). In the histochemical localization of oxygen radicals with NBT, the blue insoluble formazan and brownish DAB precipitates were larger in all plasma-treated calli than in the control samples. This difference indicated higher O_2^- production and H_2O_2 accumulation at the surface of the iris callus immediately after treatment, which shifts deep into the callus over the next hour. According to our results, plasma-derived RONS acted as an abiotic stressor upon contact with the surface of the callus, causing an oxidative burst and stress that impairs redox homeostasis. A similar accumulation of intracellular ROS immediately after plasma treatment was detected in *Arabidopsis* seedlings [108]. Generally, oxidative stress occurs when there is an imbalance between the availability of RONS and the ability of cells to neutralize or repair the damage caused by these reactive species. The content of H_2O_2 in plant material may be increased after plasma treatment or may not change significantly, as its level depends not only on production but also on the efficiency of the plant to remove toxic RONS from the system [34,108]. For example, H_2O_2 content in plasma-treated cannabis callus was not significantly different from untreated control tissue ten days after plasma treatment [34].

Direct plasma treatment represents exposure to a particular state of matter with high-energy particles that are chemically active and can have short- and long-term effects on biological processes in plant tissue [1]. According to the results obtained in this study, in response to plasma treatment, the iris calli react with complex constitutive and inducible defense mechanisms, such as the activation of key antioxidant defense enzymes and the synthesis of different types of compounds in response to physical stress. Plants have developed a number of mechanisms to protect themselves from RONS-mediated damage. There are two main pathways of ROS degradation in plants: non-enzymatic and enzymatic. Non-enzymatic systems include various secondary metabolites (antioxidants) such as phenols and flavonoids, which are capable of directly quenching ROS. Enzymatic systems, on the other hand, consist of antioxidant enzymes, including superoxide dismutase (SOD), catalase (CAT) and peroxidase (POX). SOD is the key enzyme that catalyzes the dismutation of O_2^- to H_2O_2, which is then further degraded to H_2O by CAT and POX [109]. SOD is the first step of the defense system against ROS generated in iris calli after plasma treatment. The activity of these enzymes, especially the CuZnSOD isoform, depended on the duration of plasma treatment and persisted during the first hour after plasma treatment. Increased SOD activity was found to be associated with an overproduction of ROS under various stress conditions, resulting in increased plant tolerance to environmental stress [110]. The observed changes in CuZnSOD and CAT activity in yellow iris callus corresponded with the rate of peroxide anion radical formation. Many authors have noted changes in the activity of antioxidant enzymes after CP treatment [10,34,111]. However, the changes were not uniform as they were influenced by the type of plasma device, the duration of the treatment, the working gas and the type of biological samples treated. In experiments conducted by various researchers, plasma-treated seeds and seedlings showed an increase in the activity of SOD, POX and CAT [108,112,113]. On the other hand, Rahman et al. [114] found no changes in SOD and POX activity in wheat seeds treated with plasma. SOD

and POX activity in *Arabidopsis* seeds was initially increased and then decreased with the plasma treatment time, while CAT activity was significantly decreased in plasma-treated seeds compared to untreated seeds [115]. Our previous work on meristematic cells of *Daucus carota* also showed that cold plasma induced both higher SOD and CAT activity immediately and two weeks after treatment, clearly indicating a species-specific effect of cold plasma treatments [25]. In addition, the protein level of the antioxidant enzyme isoforms was detected by immunoblot analysis with specific antibodies correlating with the CAT protein content in all plasma-treated samples immediately after treatment, with the highest values measured after the 60 s treatment compared to the control samples. The physiological response of plasma-treated iris calli measured 7d after plasma treatment was characterized by an increase in POX activity and protein content compared to control samples. It should be noted that, although immunoblot analysis provides evidence for the synthesis of the enzyme subunits, this does not necessarily correlate with the activity of the enzyme in its native form [116]. This may explain why the slight difference between the protein content (apparent decrease or increase) and the changes in enzyme activity was observed in the same CP-treated calli samples. The precise determination of the specific isoforms and their respective activity would help to clarify this point. It should also be kept in mind that the different levels of enzymatic activity are not exclusively dependent on enzyme synthesis but also on post-translational modifications [117]. In addition, the non-enzymatic antioxidant system in plants includes small molecules that control ROS homeostasis by removing, converting or neutralizing the oxidant pool, which could explain the discrepancy observed in our results [118].

There is ample evidence that the cold plasma treatment of seeds resulted in increased amounts of different specialized metabolites, such as cannabinoids in *Cannabis indica* [119], isoflavones in *Triticum pratensae* [120], and various secondary metabolites in buckwheat [121] or natural sweeteners in *Stevia rebaudiana* [122]. In nature, the biosynthesis of specialized metabolites is generally limited to certain developmental stages and periods of stress [123]. Plant callus, an unorganized, fast-growing cell mass, can be produced in almost all plant species in response to wounding or plant growth regulators [124]. Callus tissue culture has been used extensively in plant biotechnology as a tool for the genetic manipulation of plants, for studying plant metabolism and cellular development and more recently for the large-scale commercial production of valuable compounds, i.e., plant secondary metabolites, as an alternative to the direct tissue extraction of naturally occurring products that cannot be chemically synthesized. However, not all secondary metabolites present in intact plants are produced in callus cultures [69]. The synthesis of some metabolites, depending on the levels of cellular differentiation and a certain level of organization in the cell culture, is very often required for metabolite synthesis, such as for the production of mangiferin in callus cultures of *Iris raichenbachii*. In addition, the production of these metabolites depended on the type of plant growth regulators (i.e., presence of 2,4-D) in culture medium [69]. In our work, we presented for the first time the complete metabolic profile of secondary metabolites produced in *I. rechenbachii* calli. In yellow iris callus, 40 phytochemicals were identified. Among them, one flavonoid glycoside (Apigenin 6-C-hexoside-8-C-pentoside) together with eight isoflavone glycosides and six corresponding aglycones were synthesized in yellow NEC. In addition, in this work we presented the metabolic profile of the white EC of the iris, which was not treated, to compare it with the white callus obtained after CP treatment. According to the results, it is evident that the metabolic profile of white plasma-derived calli was different from that of the white EC and yellow NEC. In addition, the EC was significantly richer in secondary metabolites than the yellow NEC and plasma-treated NEC. This difference may be related

to the process of tissue differentiation during the development of somatic embryos that occurs in embryogenic tissues.

In the current study, we confirmed the synthesis of isoflavonoids in the callus of *I. rechenbachii*, which was previously reported only for the callus tissue of *I. pseudacorus* by Tarbeeva et al. [70]. Isoflavones and their glycosides are the main classes of polyphenolic compounds found in *Iris* species and were primarily recorded in the rhizome. These phytochemicals are very important as the use of iris rhizomes in both traditional and modern medicine relies on their presence in the extracts [37,38]. Many isoflavones have been named after the species of iris from which they were commonly found or were first isolated, such as tectorigenin from *Iris tectorum*, nigricin from *Iris nigricans* [125] or kashmirianin isolated from *Iris kashmiriana* [126]. The identification of isoflavones and their derivatives in our study, in the absence of standards, was based on the available literature on phytochemicals previously isolated or just identified in some iris species [94,95,127–131] and on the study of their MS fragmentation patterns (exact mass and MS^4 fragmentation).

According to our results, three flavonoids (narigenin, apigenin and acacetin) were only detected in plasma-treated callus. The synthesis of these phytochemicals was recorded in treated tissues one week and one year after CP treatment, whereas they were not present in the other two untreated calli samples (NEC and EC). While apigenin and acacetin were previously detected in irises [38,44], narigenin is characteristic of citrus fruits and was only recorded in the leaves of *I. sibirica* [63]. All these plasma-induced flavonoids have a great potential to inhibit the generation of ROS and reduce their levels as well as to fulfill antioxidant functions in tissues. We postulated that the synthesis of these compounds presents an enzymatic long-term defense response of the iris callus to ROS attack during plasma treatment. Apigenin [132], acacetin [133] and narigenin [134,135] induced in iris callus after CP treatment are excellent free radical scavengers with wide-ranging effects on human health, such as antioxidant, anti-inflammatory, anti-infection, anticancer and cardiovascular protective functions. In our study, we recorded the continuous synthesis of two isoflavonoid aglycones in *I. reichenbachii* callus, irisolidone and irilone, after CP treatment. These isoflavonoid aglycones were found in nature in rhizomes of *I. germanica* [136], endemic dwarf iris *I. adriatica* [137] and *I. pseudopumila* [138] as well as in the leaves of *I. sibirica* [63]. Irilone has strong cytotoxic and anti-inflammatory effects and also high antioxidant and estrogenic activity [139], while irisolidone possesses antioxidant, anti-inflammatory, antidiabetic and immunomodulatory activity [136,140]. This is the first report on the induction of secondary metabolites in the calli of any plant species after CP treatment without being the only stimulation of pre-existing synthesis, such as the synthesis of cannabinoids in *Cannabis sativa* callus [34] and atropine in *Datura inoxia* callus [10]. In addition, the synthesis of isoflavonoids in *I. domestica* callus is only possible after induction with $CuCl_2$ [71]. No polyphenolic phytochemicals were found in untreated callus, while induction started 7 days after $CuCl_2$ treatment and was maximally enriched 42 days after treatment and strongly decreased 49 days after elicitation treatment [71]. According to the available research results, isoflavone production in in vitro culture is influenced by various factors such as the type of culture medium but also by some physical factors (light intensity and temperature). Light, especially UV radiation, acts as a regulatory factor for the biosynthesis of isoflavonoids, as postulated for the calli culture of *Genista tinctoria* [141,142]. It is well documented that the effect of plasma on biological targets is mediated not only by chemically reactive species but also by visible light and UV radiation [7]. In this context, we postulated that the induction of the synthesis of isoflavonoids after plasma treatment in yellow iris callus was due to the physical effects of different types of light that were present in the plasma during treatment. In addition, two isoflavonoid aglycones—irigenin and iristectorigenin A/B—were synthetized in both the plasma-treated and plasma-untreated iris

callus (NEC and EC). This is the first report on the synthesis of these medicinally valuable compounds in plant callus tissue. The synthesis of the above-mentioned isoflavonoids was also recorded in the adventitious roots of *I. germanica* [62] and in the CuCl2-treated callus of *I. domestica* (previously referred as *Belamcanda chinensis*) [71].

So far all studies on the effects of plasma treatment of callus followed changes in biosynthesis up to two weeks after plasma treatment [10,34]. However, no one has yet addressed the question of long-term changes in the quality of specialized metabolites and antioxidants in plant callus due to CP treatment. In the current study, a significant decrease in isoflavonoid synthesis was observed in plasma-treated callus one year after treatment. Only constitutively present (irigenin and iristectorigenin A/B) and plasma-induced flavonoids (narigenin, apigenin and acacetin) and isoflavonoids (irisolidone and irilone) were found in the iris callus one year after plasma treatment. Polyphenols can be oxidized chemically or enzymatically by polyphenol oxidase or POX. However, new phenolic compounds can also be synthesized as a result of stress by increasing the activity of the enzyme phenylalanine ammonia lyase as a defense mechanism [143]. Therefore, follow-up studies and associated gene expression in phenylpropanoid metabolism are required to fully investigate the regulatory mechanism of CP treatment on the antioxidant capacity of yellow iris calli at the molecular level. Although the mechanism is still unclear, we hypothesize that the degradation of isoflavones results from the known ability of phenolic compounds to scavenge free radicals (antioxidant capacity). This opens up numerous possibilities for further work, including a comprehensive quantitative chemical analysis of iris calli and the changes in their antioxidant activity.

5. Conclusions

In this work, we have shown that the plasma treatment of calli acts as a stress factor that not only induces changes in morphology, physiology and growth but also contributes to increasing the content of biologically active constituents in plants. The morphological and physiological response of non-regenerative iris callus tissue induced by plasma treatment suggests that the plasma technique could be applied as an alternative and valuable approach for promoting regeneration and multiplication in plant meristematic tissue culture and as a potential elicitor for the production of various desirable secondary metabolites in plant cell and tissue culture. Here, we have shown that direct plasma treatment can significantly alter the production of secondary metabolites in *I. reichenbachii* calli, leading to qualitative changes in their phytochemical profile both in the short and long term. Therefore, our future work will involve the investigation of the molecular mechanism underlying the observed effects of CP treatment on calli.

Supplementary Materials: The following supporting information can be downloaded at https://www.mdpi.com/article/10.3390/horticulturae11070781/s1, Table S1: MS^{2-4} fragmentation data of specialized metabolites found in calli of *Iris reichenbachii*.

Author Contributions: Conceptualization, S.J., S.Ž., M.M. and N.P.; investigation, S.J., S.Ž., M.M., K.V., U.G., N.Š. and N.P.; writing—original draft preparation, S.J., S.Ž. and M.M.; writing—review and editing, S.J., S.Ž., M.M., K.V., U.G., N.Š. and N.P.; visualization, S.J., S.Ž., M.M. and N.P. All authors have read and agreed to the published version of the manuscript.

Funding: This research was funded by the Ministry of Science, Technological Development and Innovation of the Republic of Serbia, grant numbers 451-03-136/2025-03/200007, 451-03-136/2025-03/200024, 451-03-65/2024-03/200178 and 451-03-66/2024-03/200178. The results presented in this manuscript are in line with Sustainable Development Goal 2 (End Hunger) and Sustainable Development Goal 9 (Industry, Innovation and Infrastructure) of the United Nations 2030 Agenda.

Data Availability Statement: The original contributions presented in this study are included in this article. Further inquiries can be directed to the corresponding author.

Conflicts of Interest: The authors declare no conflicts of interest.

Abbreviations

The following abbreviations are used in this manuscript:

CP	Cold Plasma
RF	Radio Frequency
ROS	Reactive Oxygen Species
RONS	Reactive Oxygen and Nitrogen Species
SOD	Superoxide Dismutase
MnSOD	Manganese Superoxide Dismutase
CuZnSOD	Copper Zink Superoxide Dismutase
CAT	Catalase
POX	Peroxidase
NAA	Naphthylacetic Acid
2,4-D	2,4-Dichlorophenoxyacetic Acid
EC	Embryogenic Callus
NEC	Non-Embryogenic Callus
OC	Organogenic Callus
NBT	Nitro Blue Tetrazolium
DAB	3,3′-Diaminobenzidine
PCs	Parenchymatous Cells
MCs	Meristematic Centers

References

1. Veerana, M.; Mumtaz, S.; Rana, J.N.; Javed, R.; Panngom, K.; Ahmed, B.; Akter, K.; Choi, E.H. Recent Advances in Non-Thermal Plasma for Seed Germination, Plant Growth, and Secondary Metabolite Synthesis: A Promising Frontier for Sustainable Agriculture. *Plasma Chem. Plasma Process.* **2024**, *44*, 2263–2302. [CrossRef]
2. Bruggeman, P.J.; Iza, F.; Brandenburg, R. Foundations of atmospheric pressure non-equilibrium plasmas. *Plasma Sources Sci. Technol.* **2017**, *26*, 123002. [CrossRef]
3. Brandenburg, W.R.; Weltmann, K.-D. Atmospheric pressure plasma jets: An overview of devices and new directions. *Plasma Sources Sci. Technol.* **2015**, *24*, 064001. [CrossRef]
4. Park, G.Y.; Park, S.J.; Choi, M.Y.; Koo, I.G.; Byun, J.H.; Hong, J.W.; Sim, J.Y.; Collins, G.J.; Lee, J.K. Atmospheric-pressure plasma sources for biomedical applications. *Plasma Sources Sci. Technol.* **2012**, *21*, 043001. [CrossRef]
5. Fridman, A. Introduction to Theoretical and Applied Plasma Chemistry. In *Plasma Chemistry*; Cambridge University Press: Cambridge, UK, 2008; pp. 1–11. [CrossRef]
6. Bradu, C.; Kutasi, K.; Magureanu, M.; Puač, N.; Živković, S. Reactive nitrogen species in plasma-activated water: Generation, chemistry and application in agriculture. *J. Phys. D Appl. Phys.* **2020**, *53*, 223001. [CrossRef]
7. Bilea, F.; Garcia-Vaquero, M.; Magureanu, M.; Mihaila, I.; Mildažienė, V.; Mozetič, M.; Pawłat, J.; Primc, G.; Puač, N.; Robert, E.; et al. Non-Thermal Plasma as Environmentally-Friendly Technology for Agriculture: A Review and Roadmap. *Crit. Rev. Plant Sci.* **2024**, *43*, 428–486. [CrossRef]
8. Domonkos, M.; Tichá, P.; Trejbal, J.; Demo, P. Applications of Cold Atmospheric Pressure Plasma Technology in Medicine, Agriculture and Food Industry. *Appl. Sci.* **2021**, *11*, 4809. [CrossRef]
9. Puač, N.; Gherardi, M.; Shiratani, M. Plasma and agriculture. *Plasma Process Polym.* **2017**, e1700174. [CrossRef]
10. Tardast, Z.; Iranbakhsh, A.; Ebadi, M.; Oraghi Ardebili, Z. Corona discharge plasma stimulated production of atropine in callus of *Datura inoxia* by DNA hypomethylation and gene regulation: A novel technology for plant cell and tissue culture. *Protoplasma* **2023**, *260*, 1515–1525. [CrossRef]
11. Puač, N.; Škoro, N.; Spasić, K.; Živković, S.; Milutinović, M.; Malović, G.; Petrović, Z.L. Activity of catalase enzyme in *Paulownia tomentosa* seeds during the process of germination after treatments with low pressure plasma and plasma activated water. *Plasma Process Polym.* **2018**, *15*, e1700082. [CrossRef]
12. Bormashenko, E.; Grynyov, R.; Bormashenko, Y.; Drori, E. Cold radiofrequency plasma treatment modifies wettability and germination speed of plant seeds. *Sci. Rep.* **2012**, *2*, 741. [CrossRef] [PubMed]

13. Sivachandiran, L.; Khacef, A. Enhanced seed germination and plant growth by atmospheric pressure cold air plasma: Combined effect of seed and water treatment. *RSC Adv.* **2017**, *7*, 1822–1832. [CrossRef]
14. Lo Porto, C.; Ziuzina, D.; Los, A.; Boehm, D.; Palumbo, F.; Favia, P.; Tiwari, B.; Bourke, P.; Cullen, P.J. Plasma activated water and airborne ultrasound treatments for enhanced germination and growth of soybean. *Innov. Food Sci. Emerg.* **2018**, *49*, 13–19. [CrossRef]
15. Waskow, A.; Howling, A.; Furno, I. Mechanisms of Plasma-Seed Treatments as a Potential Seed Processing Technology. *Front. Phys.* **2021**, *9*, 617345. [CrossRef]
16. Ito, M.; Oh, J.-S.; Ohta, T.; Shiratani, M.; Hori, M. Current status and future prospects of agricultural applications using atmospheric-pressure plasma technologies. *Plasma Process Polym.* **2018**, *15*, 1700073. [CrossRef]
17. Gierczik, K.; Vukušić, T.; Kovács, L.; Székely, A.; Szalai, G.; Milošević, S.; Kocsy, G.; Kutasi, K.; Galiba, G. Plasma-activated water to improve the stress tolerance of barley. *Plasma Process Polym.* **2020**, *17*, 1900123. [CrossRef]
18. Mildaziene, V.; Ivankov, A.; Pauzaite, G.; Naucienė, Z.; Zukiene, R.; Degutyte-Fomins, L.; Pukalskas, A.; Rimantas Venskutonis, P.; Filatova, I.; Lyushkevichet, V. Seed treatment with cold plasma and electromagnetic field induces changes in red clover root growth dynamics, flavonoid exudation, and activates nodulation. *Plasma Process Polym.* **2021**, *18*, 2000160. [CrossRef]
19. Lee, H.; Kim, J.E.; Chung, M.-S.; Min, S.C. Cold plasma treatment for the microbiological safety of cabbage, lettuce, and dried figs. *Food Microbiol.* **2015**, *51*, 74–80. [CrossRef]
20. Filatova, I.I.; Lyushkevich, V.A.; Kalatskaja, J.N.; Goncharik, S.V.; Mildaziene, V.; Pauzaite, G. Influence of plasma and radiowave treatment of seeds on the accumulation of some secondary metabolites in plants. In *Proceedings of the 29 Summer School and International Symposium on the Physics of Ionized Gases; SPIG 2018, Contributed Papers & Abstracts of Invited Lectures, Topical Invited Lectures, Progress Reports and Workshop Lectures, Belgrade, Serbia, 28 August–1 September 2018*; Poparić, G., Obradović, B., Borka, D., Rajković, M., Eds.; Vinča Institute of Nuclear Sciences, University of Belgrade: Belgrade, Serbia, 2018; pp. 234–237.
21. Yodpitak, S.; Mahatheeranont, S.; Boonyawan, D.; Sookwong, P.; Roytrakul, S.; Norkaew, O. Cold plasma treatment to improve germination and enhance the bioactive phytochemical content of germinated brown rice. *Food Chem.* **2019**, *289*, 328–339. [CrossRef]
22. Judickaitė, A.; Venckus, J.; Koga, K.; Shiratani, M.; Mildažienė, V.; Žūkienė, R. Cold Plasma-Induced Changes in Stevia rebaudiana Morphometric and Biochemical Parameter Correlations. *Plants* **2023**, *12*, 1585. [CrossRef]
23. Singh, H.; Niharika; Lamichhane, P.; Gupta, R.; Kaushik, N.; Choi, E.H.; Kaushik, N.K. Enhancing crop health and sustainability: Exploring the potential of secondary metabolites and non-thermal plasma treatment as alternatives to pesticides. *Plant Biotechol. Rep.* **2023**, *17*, 803–820. [CrossRef]
24. Puač, N.; Petrović, Z.L.; Malović, G.; Đorđević, A.; Živković, S.; Giba, Z.; Grubišić, D. Measurements of voltage–current characteristics of a plasma needle and its effect on plant cells. *J. Phys. D Appl. Phys.* **2006**, *39*, 3514–3519. [CrossRef]
25. Puač, N.; Živković, S.; Selaković, N.; Milutinović, M.; Boljević, J.; Malović, G.; Petrović, Z.L. Long and short term effects of plasma treatment on meristematic plant cells. *Appl. Phys. Lett.* **2014**, *104*, 214106. [CrossRef]
26. Škoro, N.; Živković, S.; Jevremović, S.; Puač, N. Treatment of Chrysanthemum Synthetic Seeds by Air SDBD Plasma. *Plants* **2022**, *11*, 907. [CrossRef]
27. Tsuboyama, S.; Okumura, T.; Attri, P.; Koga, K.; Shiratani, M.; Kuchitsu, K. Growth control of *Marchantia polymorpha* gemmae using nonthermal plasma irradiation. *Sci. Rep.* **2024**, *14*, 3172. [CrossRef]
28. Yanagawa, Y.; Suenaga, Y.; Iijima, Y.; Endo, M.; Sanada, N.; Katoh, E.; Toki, S.; Okino, A.; Mitsuhara, I. Genome editing by introduction of Cas9/sgRNA into plant cells using temperature-controlled atmospheric pressure plasma. *PLoS ONE* **2023**, *18*, e0281767. [CrossRef]
29. Ozyigit, I.I.; Dogan, I.; Hocaoglu-Ozyigit, A.; Yalcin, B.; Erdogan, A.; Yalcin, I.E.; Cabi, E.; Kaya, Y. Production of secondary metabolites using tissue culture-based biotechnological applications. *Front. Plant Sci.* **2023**, *14*, 1132555. [CrossRef]
30. De Bellis, R.; Chiarantini, L.; Potenza, L.; Gorassini, A.; Verardo, G.; De Marco, R.; Benayada, L.; Stocchi, V.; Albertini, M.C.; Fraternale, D. High production of secondary metabolites and biological activities of *Cydonia oblonga* Mill. pulp fruit callus. *J. Funct. Foods* **2022**, *94*, 105133. [CrossRef]
31. Ozden, M. Secondary metabolite production in callus cultures of *Vitis vinifera*: Influence of genotype and sucrose concentration in the medium on antioxidant activity. *Acta Physiol. Plant* **2024**, *46*, 6. [CrossRef]
32. Lee, K.Y.; Nam, D.-H.; Jeon, Y.; Park, S.U.; Cho, J.; Gulandaz, M.A.; Chung, S.-O.; Lee, G.-J. Exploring the Production of Secondary Metabolites from a Halophyte *Tetragonia tetragonoides* through Callus Culture. *Horticulturae* **2024**, *10*, 244. [CrossRef]
33. Maqbool, M.; Ishtiaq, M.; Mazhar, M.W.; Casini, R.; Mahmoud, E.A.; Elansary, H.O. Enhancing Bioactive Metabolite Production in *Aerva sanguinolenta* Callus Cultures through Silver Nanoparticle and Salicylic Acid Elicitation. *Sustainability* **2023**, *15*, 10395. [CrossRef]
34. Darigh, F.; Iranbakhsh, A.; Oraghi Ardebili, Z.; Ebadi, M. 2022 Non-thermal plasma improved callogenesis performance and elicited the production of cannabinoids by modifying DNA methylome, expression of WRKY1 and ERF1B transcription factors, and expression of genes that contributed to the biosynthesis of cannabinoids. *Protoplasma* **2023**, *260*, 159–170. [CrossRef] [PubMed]

35. Kaššák, P. Secondary metabolites of the choosen genus Iris species. *Acta Univ. Agric. Silvic. Mendel. Brun.* **2012**, *60*, 269–280. [CrossRef]
36. Hoang, L.; Beneš, F.; Fenclová, M.; Kronusová, O.; Švarcová, V.; Řehořová, K.; Baldassarre Švecová, E.; Vosátka, M.; Hajšlová, J.; Kaštánek, P.; et al. Phytochemical Composition and In Vitro Biological Activity of *Iris* spp. (Iridaceae): A New Source of Bioactive Constituents for the Inhibition of Oral Bacterial Biofilms. *Antibiotics* **2020**, *9*, 403. [CrossRef]
37. Öztaş, F.; Türkmen, A.; Öztaş, H.; Türkmen, M. The Medical Properties of Iris and its Usage in Pharmaceutical, Perfumery and Cosmetic Industries. In *Medical Research and Its Applications*; Veeramani, V.P., Ed.; BP International: New Delhi, India, 2024; Volume 4, pp. 114–124. [CrossRef]
38. Khatib, S.; Faraloni, C.; Bouissane, L. Exploring the use of Iris species: Antioxidant properties, phytochemistry, medicinal andindustrial applications. *Antioxidants* **2022**, *11*, 526. [CrossRef]
39. Kukula-Koch, W.; Sieniawska, E.; Widelski, J.; Urjin, O.; Głowniak, P.; Skalicka Woźniak, K. Major secondary metabolites of *Iris* spp. *Phytochem. Rev.* **2015**, *14*, 51–80. [CrossRef]
40. Mizuno, T.; Okuyama, Y.; Iwashina, T. Phenolic compounds from *Iris rossii*, and their chemotaxonomic and systematic significance. *Biochem. System Ecol.* **2012**, *44*, 157–160. [CrossRef]
41. Kostić, A.Ž.; Gašić, U.M.; Pešić, M.B.; Stanojević, S.P.; Barać, M.B.; Mačukanović-Jocić, M.P.; Avramov, S.N.; Tešić, Ž.L. Phytochemical Analysis and Total Antioxidant Capacity of Rhizome, Above-Ground Vegetative Parts and Flower of Three *Iris* Species. *Chem. Biodivers.* **2019**, *16*, e1800565. [CrossRef]
42. Mykhailenko, O.; Gudžinskas, Z.; Kovalyov, V.; Desenko, V.; Ivanauskas, L.; Bezruk, I.; Georgiyants, V. Effect of ecological factors on the accumulation of phenolic compounds in Iris species from Latvia, Lithuania and Ukraine. *Phytochem. Anal.* **2020**, *31*, 545–563. [CrossRef]
43. Schütz, C.; Quitschau, M.; Hamburger, M.; Potterat, O. Profiling of isoflavonoids in *Iris germanica* rhizome extracts by microprobe NMR and HPLC-PDA-MS analysis. *Fitoterapia* **2011**, *82*, 1021–1026. [CrossRef]
44. Iwashina, T.; Mizuno, T. Flavonoids and Xanthones from the genus Iris: Phytochemistry, relationships with flower colors and taxonomy, and activities and function. *Nat. Prod. Commun.* **2020**, *15*. [CrossRef]
45. Xie, G.Y.; Zhu, Y.; Shu, P.; Qin, X.Y.; Wu, G.; Wang, Q.; Qin, M.J. Phenolic metabolite profiles and antioxidants assay of three Iridaceae medicinal plants for traditional Chinese medicine "She-gan" by on-line HPLC-DAD coupled with chemiluminescence (CL) and ESI-Q-TOF-MS/MS. *J. Pharm. Biomed. Anal.* **2014**, *98*, 40–51. [CrossRef] [PubMed]
46. Mykhailenko, O.; Korinek, M.; Ivanauskas, L.; Bezruk, I.; Myhal, A.; Petrikaitė, V.; El-Shazly, M.; Lin, G.-H.; Lin, C.-Y.; Yen, C.-H.; et al. Qualitative and Quantitative Analysis of Ukrainian Iris Species: A Fresh Look on Their Antioxidant Content and Biological Activities. *Molecules* **2020**, *25*, 4588. [CrossRef] [PubMed]
47. Reshi, Z.A.; Ahmad, W.; Lukatkin, A.S.; Javed, S.B. From Nature to Lab: A Review of Secondary Metabolite Biosynthetic Pathways, Environmental Influences, and In Vitro Approaches. *Metabolites* **2023**, *13*, 895. [CrossRef]
48. Ascough, G.D.; Erwin, J.E.; Van Staden, J. Micropropagation of iridace-A review. *Plant Cell Tissue Organ. Cult.* **2009**, *97*, 1–19. [CrossRef]
49. Al-Gabbiesh, A.; Hassawi, D.S.; Afifi, F.U. In vitro propagation of endagared Iris species. *J. Biol. Sci.* **2006**, *6*, 1035–1040. [CrossRef]
50. Bae, K.; Yoo, K.; Lee, H.; Yoon, E. Callus induction and plant regeneration of *Iris dichotoma* Pall. in endangered species. *J. Plant Biotechnol.* **2012**, *39*, 182–188. [CrossRef]
51. Safari, N.; Tehranifar, A.; Kharrazi, M.; Shoor, M. Micropropagation of endangered Iris Ferdowsii Joharchi & Memariani through callus induction. *Plant Cell Tissue Organ. Cult.* **2023**, *154*, 595–604. [CrossRef]
52. Wang, Y.; Jeknic, Z.; Ernst, R.C.; Chen, T.H.H. Efficient plant regeneration from suspension-cultured cells of tall bearded iris. *HortScience* **1999**, *34*, 730–735. [CrossRef]
53. Yabuya, T.; Ikeda, Y.; Adachi, T. In vitro propagation of Japanese garden Iris, *Iris ensata* Thunb. *Euphytica* **1991**, *57*, 77–81. [CrossRef]
54. Laublin, G.; Saini, H.S.; Cappadocia, M. In vitro plant regeneration via somatic embryogenesis from root culture of some rhizomatous irises. *Plant Cell Tissue Organ. Cult.* **1991**, *27*, 21–27. [CrossRef]
55. Liu, H.; Fan, L.; Song, H.; Tang, B.; Wang, L. Establishment of regeneration system of callus pathway *for Iris sanguinea* Donn ex Horn. *Vitr. Cell Dev. Biol. Plant* **2020**, *56*, 694–702. [CrossRef]
56. Gozu, Y.; Yokoyama, M.; Nakamura, M.; Namba, R.; Yomogida, K.; Yanagi, M.; Nakamura, S. In vitro propagation of *Iris pallida*. *Plant Cell Rep.* **1993**, *13*, 12–16. [CrossRef] [PubMed]
57. Jehan, H.; Courtois, D.; Ehret, C.; Lerch, K.; Petiard, V. Plant regeneration of *Iris pallida* Lam. and *Iris germanica* L. via somatic embryogenesis from leaves, apices and young flowers. *Plant Cell Rep.* **1994**, *13*, 671–675. [CrossRef]
58. Shimizu, K.; Nagaike, H.; Yabuya, T.; Adachi, T. Plant regeneration from suspension culture of *Iris germanica* L. *Plant Cell Tissue Organ. Cult.* **1997**, *50*, 27–31. [CrossRef]
59. Meucci, A.; Ghelardi, C.; Maggini, R.; Malorgio, F.; Chietera, G.; Mensuali, A. Micropropagation via somatic embryogenesis of *Iris pallida* Lam. Ecotypes. *Plant Cell, Tissue Organ Cult (PCTOC)* **2024**, *158*, 21. [CrossRef]

60. Boltenkov, E.V.; Rybin, V.G.; Zarembo, E.V. Cultivation of *Iris ensata* Thunb. callus tissue. *Prikl. Biokhimiia Mikrobiol.* **2004**, *40*, 244–251.
61. Boltenkov, E.V.; Zarembo, E.V. In vitro regeneration and callogenesis in tissue culture of floral organs of the genus *Iris* (Iridaceae). *Izv. Akad. Nauk. Ser. Biol.* **2005**, *2*, 174–179. [CrossRef]
62. Akashi, T.; Ishizaki, M.; Aoki, T.; Ayabe, S.-I. Isoflavonoid production by adventitious root cultures of *Iris germanica* (Iridaceae). *Plant Biotechnol.* **2005**, *22*, 207–215. [CrossRef]
63. Karpitskiy, D.A.; Bessonova, E.A.; Kartsova, L.A.; Tikhomirova, L.I. Development of approach for flavonoid profiling of biotechnological raw materials *Iris sibirica* L. by HPLC with high-resolution tandem mass spectrometry. *Phytochem. Anal.* **2022**, *33*, 869–878. [CrossRef]
64. Michalak, A.; Krauze-Baranowska, M.; Migas, P.; Kawiak, A.; Kokotkiewicz, A.; Królicka, A. *Iris pseudacorus* as an easily accessible source of antibacterial and cytotoxic compounds. *J. Pharm. Biomed. Anal.* **2021**, *195*, 113863. [CrossRef] [PubMed]
65. Para, G.; Baratti, J. Irones and precursors synthesized by *Iris sibirica* tissue culture. *Biosci. Biotechnol. Biochem.* **1992**, *56*, 1132–1133. [CrossRef] [PubMed]
66. Marner, F.J.; Simic, K.; Scholz, B.; Küster, B. Isolation and structure determination of new iridal from *Iris sibirica*. *J. Nat. Prod.* **1995**, *58*, 299–301. [CrossRef]
67. Ritzdorf, I.; Bartels, M.; Kerp, B.; Kasel, T.; Klonowski, S.; Marner, F.J. Identification of 10-desoxyiridal as an intermediate in the biosynthesis of iridals. *Phytochemistry* **1999**, *50*, 995–1003. [CrossRef]
68. Afifi, F.U.; Al-Gabbiesh, A.; Hassawi, D.S. Essential Oil Production from the Callus of Threatened Iris Species of Jordan. In *Floriculture, Ornamental, and Plant Biotechnology*; Global Science Books: London, UK, 2008; Volume V, pp. 227–233.
69. Jevremović, S.; Kristić-Milosević, D.; De Carlo, A.; Benelli, K.; Lambardi, M.; Antonić, D.; Trifunović Momchilov, M.; Lojić, M.; Subotić, A. Kultura tkiva i krioprezervacija kao metode za povećanje produkcije mangiferina kod balkanske perunike (*Iris reichenbachii* Heuffel). In Proceedings of the Zbornik radova: III Simpozijum biologa i ekologa Republike Srpske, Banja Luka, Republika Srpska, 12–14 November 2016; Golub, D., Ed.; Prirodno-matematički fakultet, Univerzitet u Banja Luci: Banja Luka, Republika Srpska, 2016; pp. 41–53.
70. Tarbeeva, D.V.; Fedoreyev, S.A.; Veselova, M.V.; Kalinovskiy, A.I.; Seletskaya, L.D.; Mazurok, T.I.; Bulgakov, V.P. Polyphenolic compounds from callus cultures of *Iris pseudacorus*. *Nat. Prod. Commun.* **2013**, *8*, 1419–1420. [CrossRef]
71. Zhu, Y.; Chen, Y.; Zhang, X.; Xie, G.Y.; Qin, M.J. Copper stress-induced changes in biomass accumulation, antioxidant activity and flavonoid contents in *Belamcanda chinensis* calli. *Plant Cell Tissue Organ. Cult.* **2020**, *142*, 299–311. [CrossRef]
72. Michalak, A.; Królicka, A. The influence of elicitors for total phenolic content in tissues of *Iris pseudacorus* plants cultured in vitro. In Proceedings of the XI Conference "In Vitro Cultures In Biotechnology and Plant Physiology", Kraków, Poland, 4–6 December 2019; Volume 61, Suppl 1. p. 57.
73. Jeknić, Z.; Jeknić, S.; Jevremović, S.; Subotić, A.; Chen, T.H.H. Alteration of flower color in *Iris germanica* L. 'Fire Bride' through ectopic expression of phytoene synthase gene (crtB) from *Pantoea agglomerans*. *Plant Cell Rep.* **2014**, *33*, 1307–1321. [CrossRef]
74. Aslanyants, L.K.; Marshavina, Z.V. Volatile oil synthesized by Iris sibirica tissue cultures. *Appl. Biochem. Microbiol.* **1979**, *15*, 581–585.
75. Mazko, O.N.; Tikhomirova, L.I.; Shcherbakova, L.V.; Bazarnova, N.G.; Karpitsky, D.A. Flavonoids of *Iris sibirica* L. grown in vitro culture. *Khimiya Rastit. Syr'ya* **2021**, *3*, 301–308. (In Russian) [CrossRef]
76. Tikhomirova, L.I.; Ilyicheva, T.N. Preparation of biotechnological raw materials of *Iris sibirica* L. with a given content of mangiferin and antiviral activity. *IOP Conf. Ser. Earth Environ. Sci.* **2020**, *421*, 022049. [CrossRef]
77. Jevremović, S.; Lojić, M.; Jeknić, Z.; Trifunović-Momčilov, M.; Antonić, D.; Petrić, M.; Subotić, A.; Radojević, L. In vitro propagation of *Iris reichenbachii* Heuff. and clonal fidelity of regenerated plants. *Bot. Serb.* **2015**, *39*, 129–136.
78. Williams, C.A.; Harborne, J.B.; Goldblatt, P. Correlations between phenolic patterns and tribal classification in the family iridaceae. *Phytochemistry* **1986**, *25*, 2135–2154. [CrossRef]
79. Williams, C.A.; Harborne, J.B.; Colasante, M. Flavonoid and xanthone patterns in bearded iris species and the pathway of chemical evolution in the genus. *Biochem. System. Ecol.* **1997**, *25*, 309–325. [CrossRef]
80. Šavikin-Fodulović, K.; Stojanović, D.; Menković, N. Fitohemijska i anatomska analiza vrste *Iris reichenbachii* Heuff. *Lek. Sirovine* **2000**, *20*, 21–26.
81. Šarić Medić, B.; Jerković-Mujkić, A.; Cubara, B.; Durmić Pašić, A.; Hanjalić Kurtović, J.; Bajrović, K.; Omeragić, E.; Dedić, M.; Bogunić, F.; Pojskic, L. Crude Extracts of Three *Iris* Species as Sources of MRSA Antimicrobial Compounds. *Eur. J. Biol.* **2024**, *83*, 182–188. [CrossRef]
82. Jevremović, S.; Subotić, A.; Radojević, L.J. In vitro morphogenesis of dwarf irises. In *Floriculture, Ornamental and Plant Biotechnology: Advances and Topical Issues*; Teixeira da Silva, J., Ed.; Global Science Books: London, UK, 2006; Volume II, pp. 551–557.
83. Jevremović, S.; Jeknić, Z.; Subotić, A. Micropropagation of irises. In *Protocols for Micropropagation of Selected Economically-Important Horticultural Plants. Methods in Molecular Biology*; Lambardi, M., Ozudogru, E.A., Jain, S.M., Eds.; Humana Press-Springer: Totowa, NJ, USA, 2012; Volume 994, pp. 291–304. [CrossRef]

84. Živković, S.; Jevremović, S.; Gašić, U.; Milutinović, M.; Petrović, Z.L.; Škoro, N.; Puač, N. Long term effects in dwarf bearded iris (*Iris reichenbachii* Heuff.) calli metabolism induced by plasma treatment. In *Proceedings of the Book of Abstracts: 9th Central European Symposium on Plasma Chemistry (CESPC-9) Joint with COST Action CA19110 Plasma Applications for Smart and Sustainable Agriculture (PlAgri), Vysoké Tatry, Slovakia, 4–9 September 2022*; Hensel, K., Cimerman, R., Lavrikova, A., Janda, M., Machala, Z., Eds.; FMFI UK: Bratislava, Slovakia, 2022; p. 137.
85. Radojević, L.; Subotić, A. Plant regeneration of *Iris setosa* Pall. through somatic embryogenesis and organogenesis. *J. Plant Physiol.* **1992**, *139*, 690–696. [CrossRef]
86. Kim, T.D.; Ahn, C.H.; Bae, K.H.; Choi, Y.E. The embryogenic competency and morphological changes during somatic embryogenesis in *Iris pseudacorus*. *Plant Biotechnol. Rep.* **2009**, *3*, 251–257. [CrossRef]
87. Murashige, T.; Skoog, F. A revised medium for rapid growth and bioassay with tobacco tissue cultures. *Physiol. Plant.* **1962**, *15*, 473–497. [CrossRef]
88. Puač, N.; Miletić, M.; Mojović, M.; Popović-Bijelić, A.; Vuković, D.; Miličić, B.; Maletić, D.; Lazović, S.; Malović, G.; Petrović, Z. Sterilization of bacteria suspensions and identification of radicals deposited during plasma treatment. *Open Chem.* **2015**, *13*, 000010151520150041. [CrossRef]
89. Betekhtin, A.; Milewska-Hendel, A.; Chajec, L.; Rojek, M.; Nowak, K.; Kwasniewska, J.; Wolny, E.; Kurczynska, E.; Hasterok, R. 5-Azacitidine Induces Cell Death in a Tissue Culture of *Brachypodium distachyon*. *Int. J. Mol. Sci.* **2018**, *19*, 1806. [CrossRef]
90. Jambunathan, N. Determination and Detection of Reactive Oxygen Species (ROS), Lipid Peroxidation, and Electrolyte Leakage in Plants. In *Plant Stress Tolerance. Methods in Molecular Biology*; Sunkar, R., Ed.; Humana Press: Totowa, NJ, USA, 2010; Volume 639, pp. 292–298. [CrossRef]
91. Dmitrović, S.; Perišić, M.; Stojić, A.; Živković, S.; Boljević, J.; Živković, J.N.; Aničić, N.; Ristić, M.; Mišić, D. Essential oils of two *Nepeta* species inhibit growth and induce oxidative stress in ragweed (*Ambrosia artemisiifolia* L.) shoots in vitro. *Acta physiol. Plant* **2015**, *37*, 64. [CrossRef]
92. Božunović, J.; Živković, S.; Gašić, U.; Glamočlija, J.; Ćirić, A.; Matekalo, D.; Šiler, B.; Soković, M.; Tešić, Ž.; Mišić, D. In vitro and in vivo transformations of *Centaurium erythraea* secoiridoid glucosides alternate their antioxidant and antimicrobial capacity. *Ind. Crops Prod.* **2018**, *111*, 705–721. [CrossRef]
93. Banjanac, T.; Dragićević, M.; Šiler, B.; Gašić, U.; Bohanec, B.; Nestorović Živković, J.; Trifunović, S.; Mišić, D. Chemodiversity of two closely related tetraploid *Centaurium* species and their hexaploid hybrid: Metabolomic search for high-resolution taxonomic classifiers. *Phytochemistry* **2017**, *140*, 27–44. [CrossRef] [PubMed]
94. Zhang, Y.Y.; Wang, Q.; Qi, L.W.; Qin, X.Y.; Qin, M.J. Characterization and determination of the major constituents in *Belamcandae* Rhizoma by HPLC–DAD–ESI-MSn. *J. Pharm. Biomed. Anal.* **2011**, *56*, 304–314. [CrossRef]
95. Chen, D.; Meng, Y.; Zhu, Y.; Wu, G.; Yuan, J.; Qin, M.; Xie, G. Qualitative and quantitative analysis of C-glycosyl-flavones of iris lactea leaves by liquid chromatography/tandem mass spectrometry. *Molecules* **2018**, *23*, 3359. [CrossRef]
96. Ibrahim, S.; Al-Ahdal, A.; Khedr, A.; Mohamed, G. Antioxidant α-amylase inhibitors flavonoids from *Iris germanica* rhizomes. *Rev. Bras. De Farmacogn.* **2017**, *27*, 170–174. [CrossRef]
97. Yu, X.; Li, M.; O'Doherty, G.A. De novo symmetric approach to the disaccharide portion of SCH-47554. *Heterocycles* **2011**, *82*, 1577–1584. [CrossRef]
98. Malović, G.; Puač, N.; Lazović, S.; Petrović, Z. Mass analysis of an atmospheric pressure plasma needle discharge. *Plasma Sources Sci. Technol.* **2010**, *19*, 034014. [CrossRef]
99. Živković, S.; Jevremović, S.; Puač, N.; Škoro, N.; Petrović, Z.L. Morphological and physiological aspects of plasma treatment-induced changes in plant cells and tissues. In Proceedings of the XXIInd International Conference on Gas Discharges and their Applications, Novi Sad, Serbia, 2–7 September 2018; Petrović, Z.L., Puač, N., Dujko, S., Škoro, N., Eds.; Serbian Academy of Sciences and Arts: Belgrade, Serbia, 2018; pp. 646–649.
100. Radojevic, L.; Landré, P. Cytological features of developing embryogenic callus and somatic embryos of *Iris pumila* L. and *Iris setosa* Pall. *G. Bot. Ital. Off. J. Soc. Bot. Ital.* **1995**, *129*, 1213–1224. [CrossRef]
101. Stanišić, M.; Raspor, M.; Ninković, S.; Milošević, S.; Ćalić, D.; Bohanec, B.; Trifunović, M.; Petrić, M.; Subotić, A.; Jevremović, S. Clonal fidelity of *Iris sibirica* plants regenerated by somatic embryogenesis and organogenesis in leaf-base culture—RAPD and flow cytometer analyses. *S. Afr. J. Bot.* **2015**, *96*, 42–52. [CrossRef]
102. Li, D.; Ji, C.; Shao, L.; Xu, T.; Chen, X.; Wang, X.; Zhang, R.; Cui, Y.; Zhang, J.; Xia, Y. An Efficient and Environmentally Friendly Strategy for Embryogenic Callus Induction and Plant Regeneration of *Iris pseudacorus* L. *J. Plant Growth Regul.* **2025**. [CrossRef]
103. Živković, S.; Jevremović, S.; Milutinović, M.; Puač, N.; Petrović, Z.L.; Škoro, N. Alteration in plant tissue morphology and physiology induced by plasma treatment. In *Program Abstracts of the Twenty-First International Summer School on Vacuum, Electron and Ion Technologies (VEIT 2019)*; Heron Press: Birmingham, UK, 2019; pp. 63–64.
104. Kurczynska, E.; Godel-Jedrychowska, K. Apoplastic and symplasmic markers of somatic embryogenesis. *Plants* **2023**, *12*, 1951. [CrossRef] [PubMed]

105. Karimi, J.; Bansal, S.A.; Kumar, V.; Pasalari, H.; Badr, A.A.; Nejad, Z.J. Effect of cold plasma on plant physiological and biochemical processes: A review. *Biologia* **2024**, *79*, 3475–3487. [CrossRef]
106. Adhikari, B.; Adhikari, M.; Park, G. The effects of plasma on plant growth, development, and sustainability. *Appl. Sci.* **2020**, *10*, 6045. [CrossRef]
107. Priatama, R.A.; Pervitasari, A.N.; Park, S.; Park, S.J.; Lee, Y.K. Current Advancements in the Molecular Mechanism of Plasma Treatment for Seed Germination and Plant Growth. *Int. J. Mol. Sci.* **2022**, *23*, 4609. [CrossRef]
108. Li, K.; Zhong, C.; Shi, Q.; Bi, H.; Gong, B. Cold plasma seed treatment improves chilling resistance of tomato plants through hydrogen peroxide and abscisic acid signaling pathway. *Free Radic. Biol. Med.* **2021**, *172*, 286–297. [CrossRef]
109. Waszczak, C.; Carmody, M.; Kangasjärvi, J. Reactive oxygen species in plant signaling. *Annu. Rev. Plant Biol.* **2018**, *69*, 209–236. [CrossRef]
110. Wang, H.; Zhang, Y.; Jiang, H.; Cao, J.; Jiang, W. A comprehensive review of effects of electrolyzed water and plasma-activated water on growth, chemical compositions, microbiological safety and postharvest quality of sprouts. *Trends Food Sci. Technol.* **2022**, *129*, 449–462. [CrossRef]
111. Zahoranová, A.; Henselová, M.; Hudecová, D.; Kaliňáková, B.; Kováčik, D.; Medvecká, V.; Černák, M. Effect of cold atmospheric pressure plasma on the wheat seedlings vigor and on the inactivation of microorganisms on the seeds surface. *Plasma Chem. Plasma Proc.* **2016**, *36*, 397–414. [CrossRef]
112. Hosseini, S.I.; Mohsenimehr, S.; Hadian, J.; Ghorbanpour, M.; Shokri, B. Physico-chemical induced modification of seed germination and early development in artichoke (*Cynara scolymus* L.) using low energy plasma technology. *Phys. Plasmas* **2018**, *25*, 013525. [CrossRef]
113. Kostoláni, D.; Ndiffo Yemeli, G.B.; Švubová, R.; Kyzek, S.; Machala, Z. Physiological responses of young pea and barley seedlings to plasma-activated water. *Plants* **2021**, *10*, 1750. [CrossRef] [PubMed]
114. Rahman, M.M.; Sajib, S.A.; Rahi, M.S.; Tahura, S.; Roy, N.C.; Parvez, S.; Reza, M.A.; Talukder, M.R.; Kabir, A.H. Mechanisms and signaling associated with LPDBD plasma mediated growth improvement in wheat. *Sci. Rep.* **2018**, *8*, 10498. [CrossRef] [PubMed]
115. Cui, D.; Yin, Y.; Sun, H.; Wang, X.; Zhuang, J.; Wang, L.; Ma, R.; Jiao, Z. Regulation of cellular redox homeostasis in Arabidopsis thaliana seedling by atmospheric pressure cold plasma-generated reactive oxygen/nitrogen species. *Ecotoxicol. Environ. Saf.* **2022**, *240*, 113703. [CrossRef] [PubMed]
116. Bailly, C.; Leymarie, J.; Lehner, A.; Rousseau, S.; Côme, D.; Corbineau, F. Catalase activity and expression in developing sunflower seeds as related to drying. *J. Exp. Bot.* **2004**, *55*, 475–483. [CrossRef] [PubMed]
117. Kokkinidis, M.; Glykos, N.M.; Fadouloglou, V.E. Catalytic activity regulation through post-translational modification: The expanding universe of protein diversity. *Adv. Protein Chem. Struct. Biol.* **2020**, *122*, 97–125. [CrossRef]
118. Soares, C.; Carvalho, M.E.; Azevedo, R.A.; Fidalgo, F. Plants facing oxidative challenges—A little help from the antioxidant networks. *Environ. Exp. Bot.* **2019**, *161*, 4–25. [CrossRef]
119. Ivankov, A.; Nauciene, Z.; Zukiene, R.; Degutyte-Fomins, L.; Malakauskiene, A.; Kraujalis, P.; Venskutonis, P.R.; Filatova, I.; Lyushkevich, V.; Mildaziene, V. Changes in growth and production of non-psychotropic cannabinoids induced by pre-sowing treatment of hemp seeds with cold plasma, vacuum and electromagnetic field. *Appl. Sci.* **2020**, *10*, 8519. [CrossRef]
120. Mildaziene, V.; Pauzaite, G.; Nauciene, Z.; Zukiene, R.; Malakauskiene, A.; Norkeviciene, E.; Stukonis, V.; Slepetiene, A.; Olsauskaite, V.; Padarauskas, A.; et al. Effect of seed treatment with cold plasma and electromagnetic field on red clover germination, growth and content of major isoflavones. *J. Phys. D Appl. Phys.* **2020**, *53*, 264001. [CrossRef]
121. Ivankov, A.; Zukiene, R.; Nauciene, Z.; Degutyte-Fomins, L.; Filatova, I.; Lyushkevich, V.; Mildaziene, V. The effects of red clover seed treatment with cold plasma and electromagnetic field on germination and seedling growth are dependent on seed color. *Appl. Sci.* **2021**, *11*, 4676. [CrossRef]
122. Judickaitė, A.; Lyushkevich, V.; Filatova, I.; Mildažienė, V.; Žūkienė, R. The potential of cold plasma and electromagnetic field as stimulators of natural sweeteners biosynthesis in *Stevia rebaudiana* Bertoni. *Plants* **2022**, *11*, 611. [CrossRef]
123. Pérez-Alonso, N.; Jiménez, E. Producción de metabolitos secundarios de plantas mediante el cultivo in vitro. *Biotechnol. Veg.* **2011**, *11*, 195–211.
124. McDonald, K.A.; Jackman, A.P.; Thorup, J.E.; Dandekar, A.M. Plant callus as a source of biochemicals. *Appl. Biochem. Biotechnol.* **1995**, *54*, 93–108. [CrossRef]
125. Al-Khalil, S.; Tosa, H.; Iinuma, M. A xanthone C-glycoside from *Iris nigricans*. *Phytochemistry* **1995**, *38*, 729–731. [CrossRef]
126. Razdan, T.K.; Kachroo, P.K.; Qadri, B.; Kalla, A.K.; Taneja, S.C.; Koul, S.K.; Dhar, K.L. Isocladrastin and kashmigenin—Two isoflavones from *Iris kashmiriana*. *Phytochemistry* **1996**, *41*, 947–949. [CrossRef]
127. Zhang, X.; Qiao, G.-X.; Zhao, G.-F.; Zhao, S.-F. Characterization of the metabolites of irisflorentin by using ultra-high performance liquid chromatography combined with quadrupole/orbitrap tandem mass spectrometry. *J. Pharm. Biomed. Anal.* **2021**, *203*, 114222. [CrossRef]
128. Fang, R.; Veitch, N.C.; Kite, G.C.; Howes, M.J.R.; Porter, E.A.; Simmonds, M.S. Glycosylated Constituents of *Iris fulva* and *Iris brevicaulis*. *Chem. Pharm. Bull.* **2011**, *59*, 124–128. [CrossRef]

129. Yehia, S.M.; Ayoub, I.M.; Watanabe, M.; Devkota H., P.; Singab, A.N.B. Metabolic profiling, antioxidant, and enzyme inhibition potential of Iris pseudacorus L. from Egypt and Japan: A comparative study. *Sci. Rep.* **2023**, *13*, 5233. [CrossRef]
130. Song, Y.Y.; Liu, Y.; Yan, Y.M.; Lu, X.F.; Cheng, Y.X. Phenolic compounds from *Belamcanda chinensis* seeds. *Molecules* **2018**, *23*, 580. [CrossRef]
131. Roger, B.; Jeannot, V.; Fernandez, X.; Cerantola, S.; Chahboun, J. Characterisation and quantification of flavonoids in *Iris germanica* L. and *Iris pallida* Lam. resinoids from Morocco. *Phytochem. Anal.* **2012**, *23*, 450–455. [CrossRef]
132. Salehi, B.; Venditti, A.; Sharifi-Rad, M.; Kregiel, D.; Sharifi-Rad, J.; Durazzo, A.; Lucarini, M.; Santini, A.; Souto, E.B.; Novellino, E.; et al. The therapeutic potential of apigenin. *Int. J. Mol. Sci.* **2019**, *20*, 1305. [CrossRef]
133. Chen, K.; Gao, Z. Acacetin, a Natural Flavone with Potential in Improving Liver Disease Based on Its Anti-Inflammation, Anti-Cancer, Anti-Infection and Other Effects. *Molecules* **2024**, *29*, 4872. [CrossRef] [PubMed]
134. Pashaei, R. Features of Apigenin, Luteolin, Hesperetin and Naringenin in Crop and Body. *Int. J. Food Sci. Nutr. Diet.* **2016**, *5*, 300–304. [CrossRef]
135. Moghaddam, H.R.; Samimi, Z.; Zachariah Moradi, S.; Little, P.J.; Xu, S.; Farzaei, M.H. Naringenin and naringin in cardiovascular disease prevention: A preclinical review. *Eur. J. Pharmacol.* **2020**, *887*, 173535. [CrossRef] [PubMed]
136. Amin, H.I.M.; Hussain, F.H.S.; Najmaldin, S.K.; Thu, Z.M.; Ibrahim, M.F.; Gilardoni, G.; Vidari, G. Phytochemistry and Biological Activities of Iris Species Growing in Iraqi Kurdistan and Phenolic Constituents of the Traditional Plant *Iris postii*. *Molecules* **2021**, *26*, 264. [CrossRef]
137. Alperth, F.; Mitić, B.; Mayer, S.; Maleš, Ž.; Kunert, O.; Hruševar, D.; Bucar, F. Metabolic profiling of rhizomes of native populations of the strictly endemic Croatian species Iris adriatica. *Plant Biosyst.* **2019**, *153*, 317–324. [CrossRef]
138. Conforti, F.; Menichini, F.; Rigano, D.; Senatore, F. Antiproliferative activity on human cancer cell lines after treatment with polyphenolic compounds isolated from *Iris pseudopumila* flowers and rhizomes. *Z. Naturforsch C.* **2009**, *64*, 490–494. [CrossRef]
139. Lutter, S.; Schmalbach, K.; Esch, H.L.; Lehmann, L. The isoflavone irilone contributes to the estrogenic potential of dietary supplements containing red clover. *Arch. Toxicol.* **2014**, *88*, 309–321. [CrossRef]
140. Kang, K.A.; Zhang, R.; Piao, M.J.; Ko, D.O.; Wang, Z.H.; Kim, B.J.; Park, J.W.; Kim, H.S.; Kim, D.H.; Hyun, J.W. Protective effect of irisolidone, a metabolite of kakkalide, against hydrogen peroxide induced cell damage via antioxidant effect. *Bioorg. Med.Chem.* **2008**, *16*, 1133–1141. [CrossRef]
141. Tůmová, L.; Tůma, J. The efect of UV light on isofavonoid production in *Genista tinctoria* culture in vitro. *Acta Physiol. Plant* **2011**, *33*, 635–640. [CrossRef]
142. Vidya, N.; Saravanan, K.; Halka, J.; Kowsalya, K.; Preetha, J.S.Y.; Gurusaravanan, P.; Radhakrishnan, R.; Nanthin, A.U.R.; Arun, M. An insight into in vitro strategies for bioproduction of isoflavones. *Plant Biotechnol. Rep.* **2021**, *15*, 717–740. [CrossRef]
143. Heredia, J.B.; Cisneros-Zevallos, L. The effect of exogenous ethylene and methyl jasmonate on pal activity, phenolic profiles and antioxidant capacity of carrots (*Daucus carota*) under different wounding intensities. *Postharvest Biol. Technol.* **2009**, *51*, 242–249. [CrossRef]

Disclaimer/Publisher's Note: The statements, opinions and data contained in all publications are solely those of the individual author(s) and contributor(s) and not of MDPI and/or the editor(s). MDPI and/or the editor(s) disclaim responsibility for any injury to people or property resulting from any ideas, methods, instructions or products referred to in the content.